Channel Estimation Techniques for WCDMA Communication Systems

XiBin Han

A Thesis

in

The Department

of

Electrical and Computer Engineering

Presented in Partial Fulfillment of the Requirements

for the Degree of master of Applied Science at

Concordia University

Montreal, Quebec, Canada

December 2004

Your file Votre référence
ISBN: 0-494-04374-1
Our file Notre référence
ISBN: 0-494-04374-1

ABSTRACT

Channel Estimation Techniques for WCDMA Communication Systems

Xi Bin Han

Wideband code division multiple access (WCDMA) technique has received a great deal of research attention over the past years due to its extensive applications in the third-generation (3G) wireless communication systems which are believed to dominate the global telecommunication market very soon. It is well known that signals transmitted in wireless channels suffer from multipath fading, seriously degrading the transmission performance. As one of the major signal processing tasks in a WCDMA receiver, channel estimation plays a crucial role in the realization of 3G communication systems in order to cope with multipath fading.

This thesis focuses on the study of efficient channel estimation techniques for WCDMA communication systems. Some background material pertaining to wireless multipath propagation and WCDMA systems is first presented. The maximum-likelihood principle based data-aided channel estimation techniques are then investigated, resulting in two new estimation methods using pilot and information symbols. The first method combines the pilot-assisted and the decision-directed estimation schemes, yielding a much better estimation result compared to each of the two schemes alone. The second technique corresponds to an adaptive channel estimation scheme in which a new update mechanism

using a variable step-size is proposed. A theoretical analysis of the mean square error of the least mean square (LMS) algorithm is conducted, showing the superiority of a variable step-size update scheme in convergence speed over the conventional constant step-size algorithm. The proposed scheme is not only able to increase the convergence speed but also can decrease the steady-state error of the adaptive estimation filter to a certain degree.

The bit-error rate (BER) performance of both downlink and uplink of the WCDMA systems using the proposed channel estimation techniques is evaluated through extensive computer simulations for different mobile velocities, confirming the improved estimation accuracy of the proposed methods for both slow to fast fading channels in comparison with some of the existing techniques.

ACKNOWLEDGEMENTS

It is with the utmost sincerity that I would like to express my thanks to my thesis supervisor, Dr. Wei-Ping Zhu, for his constant guidance and stimulating suggestions through the various stages of the thesis development. I am grateful for his extremely careful and thorough review of my thesis. I would also like to thank all the professors with whom I have interacted during my studies at Concordia University. Last but not least, I would like to thank my family and friends. Their love, trust and support accompany with me throughout all these years. I am grateful to all of you.

Contents

LIST OF TABLES

LIST OF FIGURES

LIST OF ABBREVIATIONS AND SYMBOLS

3G	Third-Generation
AWGN	Additive White Gaussian Noise
BER	Bit Error Rate
CDM	Code-Division Multiplexed
CDMA	Code Division Multiple Access
DA	Data-Assisted
DD	Decision-Directed
DPCCH	Dedicated Physical Control Channel
DPDCH	Dedicated Physical Data Channel
FDMA	Frequency Division Multiple Access
IFFT	Inverse Fast Fourier Transform
LMS	Least Mean Squared
MAP	Maximum A Posteriori
ML	Maximum Likelihood
MMSE	Minimized Mean Square Error
MSE	Mean Square Error
NDA	Non-Data-Assisted
PA	Pilot-Assisted
PADD-WMSA	Pilot-Assisted WMSA and Decision-Directed

QCE	Quality of Channel Estimation
QPSK	Qudrature Phase Shift Keying
SNR	Signal-to-Noise Ratio
TDM	Time-Division Multiplexed
TDMA	Time Division Multiple Access
WCDMA	Wideband Code Division Multiple Access
WMSA	Weighted Multi-Slot Averaging

A_d Data power Gain

A_p Pilot power Gain

a_i The i^{th} attenuation factor

c Light speed

D Unit time delay

D_B Bhattacharyya bound

$E[\cdot]$ Expected value of a random variable

e_n Error signal

f_c Carrier frequency

f_{cp} Transmitter pilot chip frequency

f_m Maximum Doppler frequency

$\mathbf{g} = [g_{-N},...,g_0,...,g_N]^T$ 2N+1 ideal time-invariant filter coefficients vector

g_k Ideal infinite-duration time-invariant filter,

$h(\cdot)$ Channel impulse response

$\tilde{h}(\cdot)$ Unfiltered instantaneous channel impulse response

$\hat{h}(\cdot)$ Estimated channel impulse response

$h_l(\cdot)$ The l^{th} path complex channel impulse response

$\tilde{h}_l(\cdot)$ The l^{th} path unfiltered complex channel response

$\tilde{\mathbf{h}}_n = [\tilde{h}_{n+N},...,\tilde{h}_n,...,\tilde{h}_{n-N}]^T$ Unfiltered 2N+1 channel coefficients vector

L Total paths of wireless communication multipath channel

l One path of wireless communication multipath channel

$r(\cdot)$	Received signal at the receiver
$r_l(\cdot)$	Received l^{th} path signal
S	Average received signal power
SF	Spreading factor
$S_m(f)$	Rayleigh fading power spectrum
$s_e(\cdot)$	Complex envelop of $s(\cdot)$
$s_R(\cdot)$	The magnitude of envelop $s(\cdot)$
T_c	Chip duration of the spreading sequence
T_s	Symbol period
$v(t)$	Filtered noise
$v_e(\cdot)$	Channel estimation error
v_m	Velocity of the mobile relative to the base station
w_{opt}	Optimal closed-form solution in the MMSE sense
α_i	Real-valued linear tap coefficient or weighting factor
$\delta(\cdot)$	Delta function
ε_n	Mean square error at the n^{th} instant
ε_n^r	Reducible channel estimation error
γ_c	SNR at chip level
λ	Wavelength of the carrier waveform
μ	Step-size

ρ_n	Irreducible channel estimation error
σ^2	Variance of Gaussian noise
σ_h^2	Estimate channel coefficient mean power
σ_ρ^2	Mean power of ρ_n
ζ	Quality of Channel Estimation (QCE)
ζ_d	QCE of downlink,
ζ_u	QCE of uplink,
$\Re\{\cdot\}$	Real part of $\{\cdot\}$
$(\cdot)^*$	Complex conjugate
$(\cdot)^H$	Complex conjugate transpose

Chapter 1

Introduction

1.1 Wireless Digital Communication Systems

A wireless digital communication system involves transmission of information in digital form from one point to another through a physical radio channel. Fig. 1.1 illustrates a general block diagram for a wireless communication system. Basically, the encoder, the baseband modulator and the radio frequency (RF) modulator constitute the transmitter, and the receiver consists of the RF demodulator/downconverter, the baseband demodulator and the decoder. The encoder usually comprises both the source encoder and the channel encoder, the former converting an analog signal to a digital one possibly with compression and the later carrying out forward error control (FEC) coding. The baseband modulator performs a number of tasks in relation to the formation and processing of a real or complex baseband signal, typically, including the binary-to-constellation mapping, pulse shaping, the in-phase (I) and the quadrature (Q) multiplexing etc., depending on the modulation scheme chosen. The RF modulator is to upconvert the baseband signal to a high frequency passband signal for radio transmission. The communication channel or the transmission media can be wired, wireless or optical fibre. The transmitted signal normally suffers from an additive white Gaussian noise (AWGN) no matter what transmission media is used. In wireless channels, however, there often exists multipath fading which becomes a major distortion source degrading the transmission performance.

At the receiver, a reverse process of the operations in the transmitter is implemented, which includes the RF demodulator/downconverter for converting the RF signal back to the baseband version, the baseband demodulator carrying out many signal processing tasks in order to recover the original information sequence or bitstream, and the decoder for channel and source decoding.

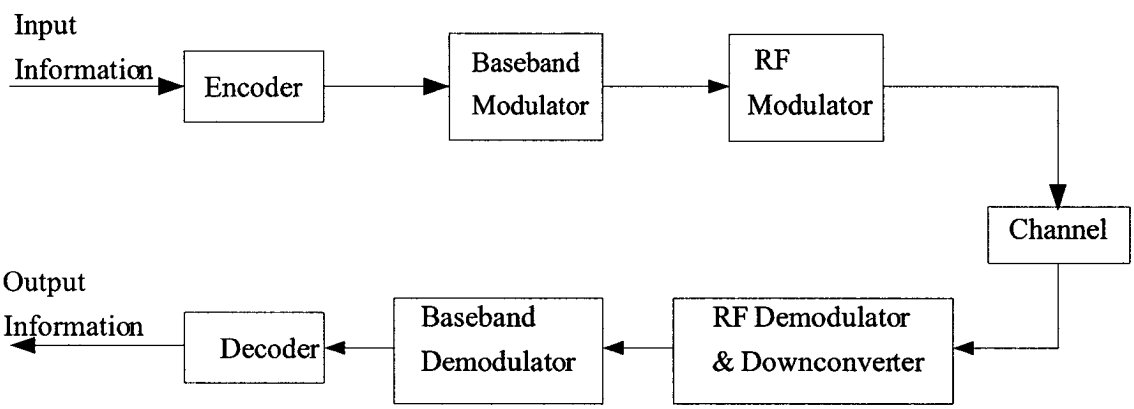

Fig.1.1 Physical communication model

Due to the AWGN and the imperfection of the channel, a communication system may produce bit errors. That is, not all information bits can be correctly recovered in the receiver. This bit error problem could be worse in wireless communication systems, where many obstacles such as buildings, hills, trees etc. cause multipath propagation of the signal as illustrated in Fig. 1.2. It is easy to see that the signals reflected by these obstacles/objects may arrive at the receiver at different times with different amplitude and phase distortions known as multipath fading. Multipath fading is one of the most commonly addressed issues in wireless communications. Many modulation schemes and receiver structures have been proposed to tackle this issue.

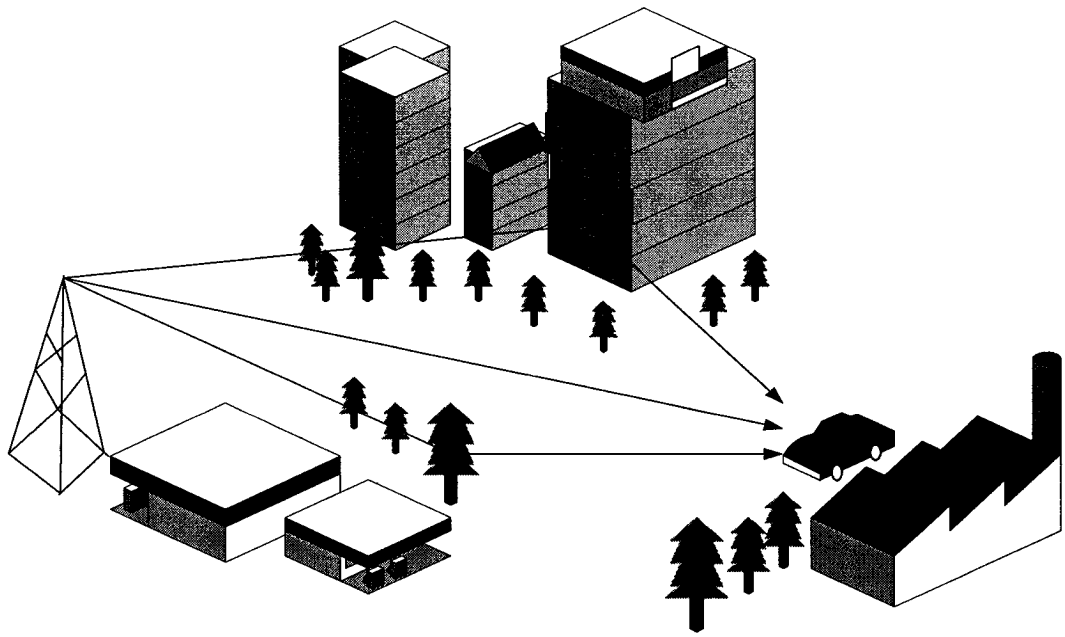

Fig. 1.2 Multipath propagation channel

1.2 WCDMA and Rake Receiver

Code division multiple access (CDMA) technique has been extensively used in the second-generation (2G) mobile communication systems over the past decade. It uses a very large bandwidth to transmit a spread signal that is generated by multiplying the information bits with a signature code or spreading sequence. In the receiver of a CDMA system, the same signature code as used by the transmitter along with a time-domain correlation operation is employed to detect the original information signal. As each user is assigned a specific spreading sequence and the spreading sequences for different users are orthogonal, the information bits from different users can be identified.

Due to its use of large bandwidth, CDMA is able to offer a number of advantages over

the traditional time division multiple access (TDMA) and frequency division multiple access (FDMA) techniques. For example, the propagation paths of a wideband signal over wireless channel can be resolved with a higher accuracy than those of a narrow-band signal, implying a better transmission performance for large bandwidth signals in multipath fading environments. The large capacity and easy deployment of a CDMA system have also made it more advantageous relative to other multiple access systems. As the third-generation (3G) wireless communication systems will dominate the global telecommunication market very soon, it is believed that CDMA, especially wideband CDMA (WCDMA), will become a major modulation and multiplexing technique.

Multipath fading in wireless communication systems causes multiple replicas of the transmitted signal, each delayed in time and attenuated in amplitude. If these multipath components are delayed relative to the direct path in time by more than one chip duration, they can be regarded as uncorrelated noise and can be neglected after dispreading provided that the processing gain is large enough. However, since the multipath components carry the delayed versions of the information signal, they can be exploited to enhance the signal-to-noise ratio (SNR) of the wireless channel and therefore to improve the bit error rate (BER) performance of the system. Rake receiver is often used to deal with these multipath components of the original information signal, which consists of a number of fingers, each aimed at one propagation path and estimating the spread delay and the attenuation of the path. Using Rake receiver, the multipath components can be resolved and aligned in time as well as boosted in amplitude and hence, they can be

combined to enhance the power of the received signal significantly.

The Rake receiver technique was first proposed by Price and Green to cope with multipath fading [4], [7]. It has been specified in the WCDMA standard and is being widely used in the current 2G and 2.5G mobile communication systems and products. Fig. 1.3 shows a three-finger Rake receiver often used in WCDMA systems. The input of the Rake is from the front-end radio frequency (RF) demodulator which has down-converted the received high-frequency signal to the baseband complex signal with In-phase (I) and Qudrature (Q) components. Code generators are used to generate various known signature codes for the dispreading of spread chip-rate signal. Correlators perform multiplication and integration on the chip signals for the detection of transmitted bit-rate data symbols. Note that the three fingers carry out the detection of the multipath replicas of the information signal, which arrive at different times with different gains. One of the most important tasks in Rake receiver is to estimate the channel gain and the spread delay of each of the fading paths. The pilot symbols specified in the standard are normally used for channel estimation. The estimated complex channel gain is then used to correct the phase of the detected data symbols for each path in Phase Rotator. The channel-compensated data symbols from different paths are delayed properly and aligned for Rake combining. The Rake combiner generates the enhanced I and Q signals which will be used for decision and decoding in the next stage of the receiver. The matched filter in the Rake receiver is employed to search for the spread delay for each of the fading paths. In this study, we will focus on the channel estimation part of the Rake

receiver with emphasis on the estimation of the complex channel gain using pilot symbols.

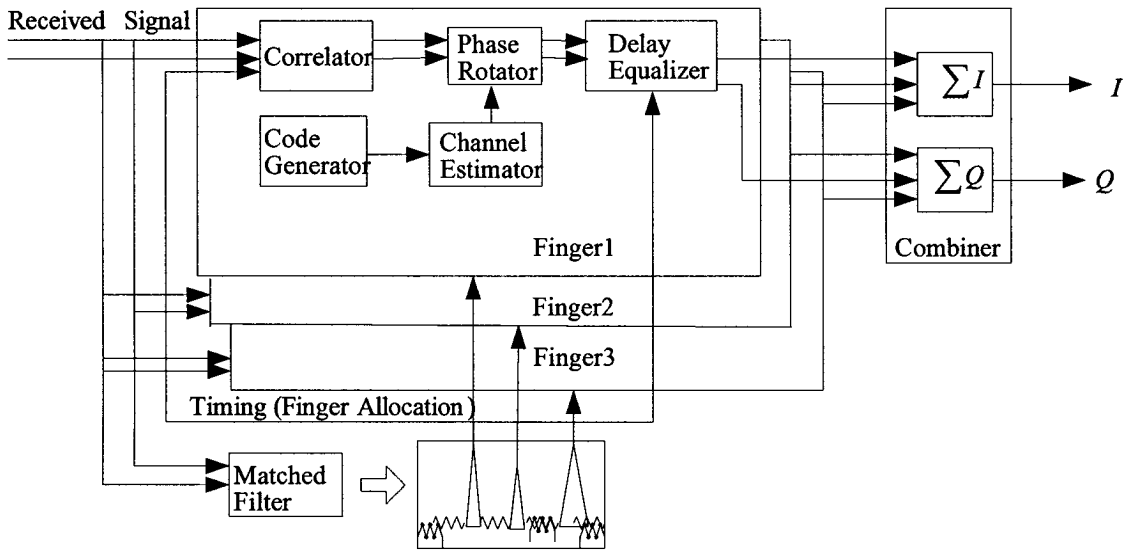

Fig. 1.3 Block diagram of the WCDMA Rake receiver

1.3 WCDMA Channel Estimation

Channel estimation in wireless communication systems is a typical signal processing task with an objective of obtaining the time-varying channel characteristic or the complex channel gain from the received noisy pilot or data symbols.

Many algorithms have been proposed for the estimation of time-varying channel characteristics in recent years [14~16], [22~30]. Broadly speaking, these algorithms can be classified as data-aided (DA) and non-data-aided (NDA) techniques depending whether or not a training sequence is required. In general, the DA techniques are capable of providing more accurate and reliable estimation results while the NDA methods are more efficient in terms of consuming the channel resource. In WCDMA systems, pilot

symbols have been allocated, which can readily be used for channel estimation. In this thesis, therefore, we concentrate on the class of data-aided estimation methods using pilot symbols. Although a considerable amount of work has been done in this area, yet very few of the existing methods can be directly applied to a practical wireless communication system either because of the high implementation complexity/cost of these methods or their low suitability for a real wireless environment where the channel experiences a wide range of fading and degradation.

1.4 Objective and Organization of the Thesis

The key to the success of WCDMA communication systems lies in the design and development of a powerful and cost-effective Rake receiver. As one of the major tasks in Rake receiver, channel estimation plays a crucial role in the realization of 3G mobile communication systems. The objective of this thesis is to develop efficient standard-compatible channel estimation techniques for WCDMA systems. Our research focus is on the investigation of data-aided estimation methods using pilot and information symbols, since this class of techniques is able to provide reliable and accurate estimation results. The rest of the thesis is organized as follows.

Chapter 2 provides background material on wireless communication fading channels. The modelling, distribution and classification of fading channels are discussed. In particular, Clarke's model, one of the most commonly used models for small-scale Rayleigh fading channels, is analyzed and simulated for different mobile velocities, showing some

simulation results helping understanding of the nature of Rayleigh fading channels.

Chapter 3 serves as brief overview of the existing channel estimation techniques including the maximum likelihood (ML) estimation principle, the pilot-assisted methods and the information symbol based decision-directed algorithms. The configurations of WCDMA downlink and uplink physical channels are also described, showing the time-multiplexed pilot symbol structure of the downlink and the code-multiplexed structure of the uplink as well as the equivalence of the BER performance for the two links. Furthermore, the upper bound of the BER performance, namely Bhattacharyya bound is also shown in this chapter.

Chapter 4 presents a non-adaptive channel estimation scheme for both the downlink and the uplink of WCDMA systems. The new technique is based on so-called weighted multi-slot averaging (WMSA) channel estimation approach and combines the pilot-assisted and decision-directed schemes. A simulation study of the proposed estimation method is carried out, showing a superior estimation performance over the basic WMSA approach.

In Chapter 5, a variable step-size adaptive channel estimation scheme is presented. A transversal adaptive filter is studied in conjunction with the least mean squared (LMS) algorithm for the purpose of channel estimation. The convergence speed as well as the steady state error of the proposed adaptive scheme is analyzed. It is shown that the proposed variable step-size adaptive estimation algorithm has a fast convergence rate given the length of the adaptive transversal filter. Simulation results showing the

superiority of the proposed method over traditional fixed step-size adaptive techniques are also presented.

Finally in Chapter 6, some concluding remarks concerning the merits of the proposed channel estimation techniques as well as suggestions for future study are provided.

Chapter 2

Wireless Communication Channels

As mentioned in the previous chapter, pass-band signals transmitted over wireless channels undergo multipath fading, especially in mobile wireless environments, seriously degrading the transmission performance of communication systems. Tremendous efforts have been made to tackle the multipath fading over the last decade. A great deal of research attention has been paid to the characterization of mobile wireless channels. A common solution to the multipath fading problem is to design the transmitter and receiver as well as to select a modulation scheme properly such that the multipath fading effect can be well compensated. To this end, an appropriate characterization of wireless channels or radio propagation paths is necessary. It is particularly important in developing coherent receiver algorithms for wideband communication systems.

In this chapter, we will first investigate and classify different wireless mutipath fading channels. We will then look into large- and small-scale fading mechanisms with emphasis on the study of a commonly used fading channel model, i.e., Clarke's model. Some simulation results relating to the model of Clarke for different mobile velocities will also be presented.

2.1 Classification of Multipath Fading Channels

There are two types of fading in mobile wireless communication channels, namely,

large-scale fading and small-scale fading. Large-scale fading represents the average attenuation of the signal power or the average path loss due to the distance between the receiver and the transmitter. Small-scale fading refers to the rapid fluctuation of the amplitude and phase of a radio signal over a short period of time or travel distance. Small-scale fading manifests itself in two mechanisms—time-spreading of the signal and the time-variant behaviour of the channel. The motion of the mobile terminal causes a variable propagation path, resulting in the time-varying characteristic of the channel. Some factors in the radio propagation channel may give rise to small-scale fading. These factors include:

- Multiple propagation paths ? the transmitted signal arrives at the receiver via different propagation paths. In most areas, particularly in urban areas, the mobile terminal is always surrounded by buildings and other structures. The reflections by the ground and surrounding objects cause multipath. The reflective signals arrive at the receiver from different directions with different propagation delays. Therefore, the received signal is a superposition of a number of waves having random amplitudes, phases, and angles of arrival._
- Bandwidth of the transmitted signal ? when the bandwidth of the transmitted signal is greater than that of the multipath channel, the received signal will be distorted while its amplitude will not fade too much, implying that the small-scale fading is not significant. Otherwise, if the transmitted signal has a narrower bandwidth relative to the channel, the amplitude of the received signal may change

rapidly without causing time-domain distortion.

- Motion of mobile terminal and/or surrounding objects ? the motion of mobile terminal relative to base station results in a frequency modulation of the multipath components. This phenomenon is known as Doppler shift, its sign depending on whether the mobile receiver is moving toward or away from the base station. On the other hand, moving objects over wireless channels also induce a time-varying Doppler shift on multipath components. If surrounding objects move at a greater speed than the mobile, the small-scale fading will be dominated by the moving objects instead of the mobile terminal. Otherwise, the motion of surrounding objects can be ignored and only the mobile's motion needs to be considered. The maximum Doppler shift is given by [8]

$$f_m = v_m / \lambda = v_m \frac{f_c}{c} \tag{2.1}$$

where

f_m: maximum Doppler frequency,

v_m: velocity of the mobile relative to the base station,

λ: wavelength of the carrier waveform,

f_c: carrier frequency,

c : light speed.

Fig. 2.1 shows the classification of wireless communication fading channels. Note that the small-scale fading channels can be further classified in frequency domain or time

domain.

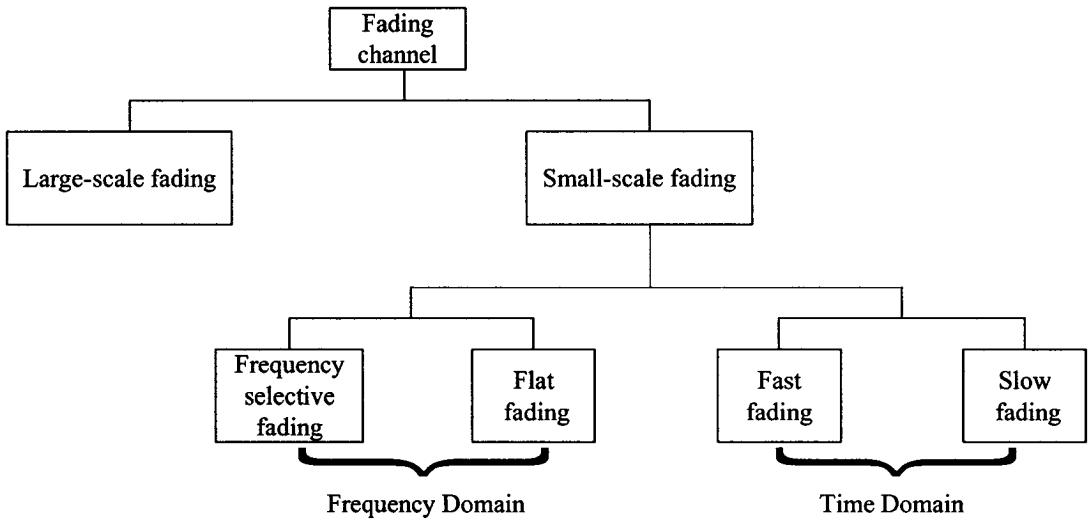

Fig. 2.1 Fading channel classification

In the frequency domain, it is divided into flat fading and frequency selective fading. Flat fading occurs when the mobile wireless channel has a constant gain and a linear-phase characteristic over a frequency band that is greater than the bandwidth of the received signal. Otherwise, if the bandwidth of the constant-gain and linear-phase channel is smaller than that of the transmitted signal, the frequency selective fading takes place. The fast and slow fading categories are defined in time domain according to the time-varying characteristic of the channel. Whether a channel undergoes fast or slow fading depends on the velocity of the mobile (or the objects in the channel) and the duration of the information symbol. In a fast fading situation, the channel response changes rapidly within the symbol duration. The signal distortion in frequency domain due to fast fading increases with the increase of the Doppler shift relative to the bandwidth of the transmitted signal. In the slow fading case, the channel impulse response changes at a rate

much lower than the base-band signal rate. The time delay and the coherence bandwidth are used to describe the time dispersion nature of the channel. In the mean time, the Doppler shift and the coherence time determine the time variant behaviour of the channel. Using complex notation, the transmitted signal can be written as

$$s(t) = \Re\{s_e(t)e^{j2pf_c t}\} \tag{2.2}$$

where

$\Re\{\cdot\}$ denotes the real part of $\{\cdot\}$,

$s_e(t)$ is the complex envelop of $s(t)$, and it can be expressed as

$$s_e(t) = |s_e(t)|e^{j\phi(t)} = s_R(t)e^{j\phi(t)} \tag{2.3}$$

with $s_R(t)$ and $\phi(t)$ being the magnitude and the phase of the envelop, respectively. For a purely phase-modulated signal, such as the WCDMA signal, $s_R(t)$ is a constant, and in general, it varies slowly compared to the carrier frequency.

Note that $s_e(t)$ will be distorted by a complex multiplicative factor $\alpha_s(t)e^{-j\theta(t)}$ when the signal is transmitted in a fading channel. Thus, the distorted signal can be written as $\alpha_s(t)e^{-j\theta(t)}s_e(t)$. Further, its magnitude $\alpha_s(t)s_R(t)$ can be expressed in terms of three positive components [47], namely,

$$\alpha_s(t)s_R(t) = m(t) \times r_0(t) \times s_R(t) \tag{2.4}$$

where $m(t)$ and $r_0(t)$ represent, respectively, the large-scale fading and the small-scale fading components of the envelope. The former is often referred to as the local mean or the log-normal fading since its probability density function is log-normal [1], and the later referred to as multipath small-scale fading. In this thesis, we concentrate on the

category of small-scale fading.

2.2 Channel Model for Wireless Communication Systems

2.2.1 Multipath Channel Response

The general form of the input/output relationship of a continuous-time linear time-varying channel with additive noise is given by

$$y(t) = \int_{-\infty}^{+\infty} h(t,\tau)x(t-\tau)d\tau + n(t) \tag{2.5}$$

where

$x(t)$: channel input,

$y(t)$: channel output,

$h(t,\tau)$: channel impulse response,

$n(t)$: additive Gaussian noise.

As the time-varying impulse response $h(t,\tau)$ can be regarded as a 2-D random process, (2.5) represents actually a probabilistic model. It is very difficult to deal with this model due to the random and time-varying nature of the channel. For the interest of practical applications, the random process model can be described by using a parametric model with physically meaningful parameters/quantities, such as delays and Doppler frequencies.

In WCDMA communication systems, the channel can be modeled as the superposition of a number of paths [43]. Assuming that a total of L paths can be resolved, the impulse response of the time-varying channel can be simplified as

$$h(t,\tau) = \sum_{l=0}^{L-1} h_l(t)\delta(\tau - \tau_l(t)) \tag{2.6}$$

where

$h_l(t)$:channel impulse response associated with the l^{th} path,

$\tau_l(t)$:time delay associated with the l^{th} path.

Very often the path delays do not vary significantly over a symbol period such that the time variation of $h_l(t)$ can be fitted by a linear combination of sinusoids [43], [44] as given below,

$$h_l(t) = \sum_{p=0}^{P-1} h_{l,p} e^{j2pf_{l,p}t} \tag{2.7}$$

Assuming a constant delay and combining (2.6) with (2.7), the channel response can be rewritten as

$$h(t,\tau) = \sum_{q=0}^{Q-1} h_q e^{j2pf_q t}\delta(\tau - \tau_q) \tag{2.8}$$

where $Q = PL$. Using (2.8), the channel is modelled as a superposition of Q paths, each determined by the triplet (h_q, τ_q, f_q).

2.2.2 Clarke's Model

The multipath fading channel can be modelled as either a stochastic or a deterministic process. Although a deterministic model is easier to use, it is only suitable for a class of fading channels with a constant delay assumption. The 2-D stochastic modelling is a more general way that is able to give a global characterization of a time-varying fading

channel and has more degrees of freedom which can be used to better describe the random nature of the channel. There are several probability distributions which can be considered in statistical modeling of the fading channel.

Clarke has developed a statistical model for describing the multipath characteristics of a wireless channel [9]. The model assumes a fixed transmitter with a vertically polarized antenna. The electromagnetic field incident on the mobile antenna is assumed to be comprised of N azimuthal plane waves with arbitrary phases and arbitrary azimuthal angles of arrival, each wave having equal average amplitude. It should be noted that the equal average amplitude assumption is for the case of no direct propagation path.

Fig. 2.2 shows the transmitted waves incident on a mobile travelling at a velocity v. The angles of arrival of the waves are measured in the x-y plane with respect to the direction of motion. Each wave that is incident on the mobile undergoes a Doppler shift due to the motion of the mobile terminal.

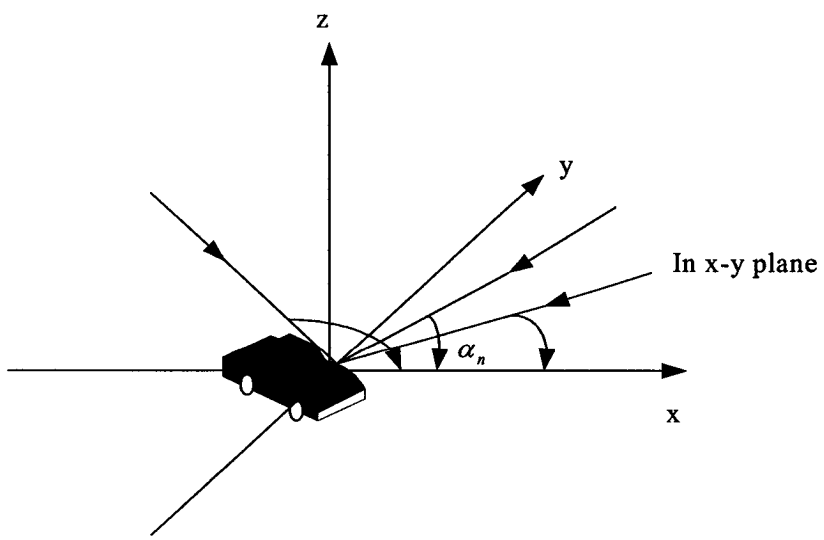

Fig. 2.2 Plane waves arriving at random angles

For the n-th wave arriving at an angle α_n with respect to the x-axis, the Doppler shift is given by

$$f_n = \frac{v}{\lambda}\cos\alpha_n \tag{2.9}$$

The vertically polarized plane waves arriving at the mobile have electric (E) and magnetic (H) field components as given by

$$E_z = E_0 \sum_{n=1}^{N} C_n \cos(2pf_c t + \theta_n) \tag{2.10}$$

$$H_x = -\frac{E_0}{\eta} \sum_{n=1}^{N} C_n \sin\alpha_n \cos(2pf_c t + \theta_n) \tag{2.11}$$

$$H_y = -\frac{E_0}{\eta} \sum_{n=1}^{N} C_n \cos\alpha_n \cos(2pf_c t + \theta_n) \tag{2.12}$$

where E_0 is the amplitude of the average E-field, C_n is a random variable representing the amplitude of the individual waves, η is the intrinsic impedance of free space. The random phase of the n-th arriving component θ_n is given by

$$\theta_n = 2\pi f_n t + \phi_n \tag{2.13}$$

The amplitudes of the E- and H-fields are normalized such that the ensemble average of C_n is unity.

Since the Doppler shift is very small compared to the carrier frequency, the three field components can be modeled as narrow-band random processes and they can be approximated by Gaussian random variables if N is sufficiently large. The phases are assumed to have a uniform distribution in $[-\pi, \pi]$. The E-field can be expressed in a quadrature form using I and Q components,

$$E_z(t) = T_c(t)\cos 2\pi f_c t - T_s(t)\sin 2\pi f_c t \tag{2.14}$$

where

$$T_c(t) = E_0 \sum_{n=1}^{N} C_n \cos(2pf_n t + \phi_n) \tag{2.15}$$

and

$$T_s(t) = E_0 \sum_{n=1}^{N} C_n \sin(2pf_n t + \phi_n) \tag{2.16}$$

The above $T_c(t)$ and $T_s(t)$ are uncorrelated Gaussian random processes with a zero mean and variance of $E_0^2/2$. The amplitude of the received E-field, $E_z(t)$, that is given by

$$|E_z(t)| = \sqrt{T_c^2(t) + T_s^2(t)} \tag{2.17}$$

has, therefore, a Rayleigh distribution.

In Clarke's model, the spectrum of the Rayleigh fading channel is centered at the carrier frequency and limited in the range of $f_c \pm f_m$. The output spectrum is then given by

$$S_m(f) = \frac{k_c}{pf_m\sqrt{1-\left(\frac{f-f_c}{f_m}\right)^2}} \tag{2.18}$$

where k_c is a constant related to the parameters of antenna and the direction of arrival of the transmitted waveform [1]. Fig. 2.3 shows the spectral density of the resulting RF signal due to Doppler shift. It is clear that the Doppler shift is symmetric about the carrier frequency f_c, and the span of the spectrum is $2f_m$.

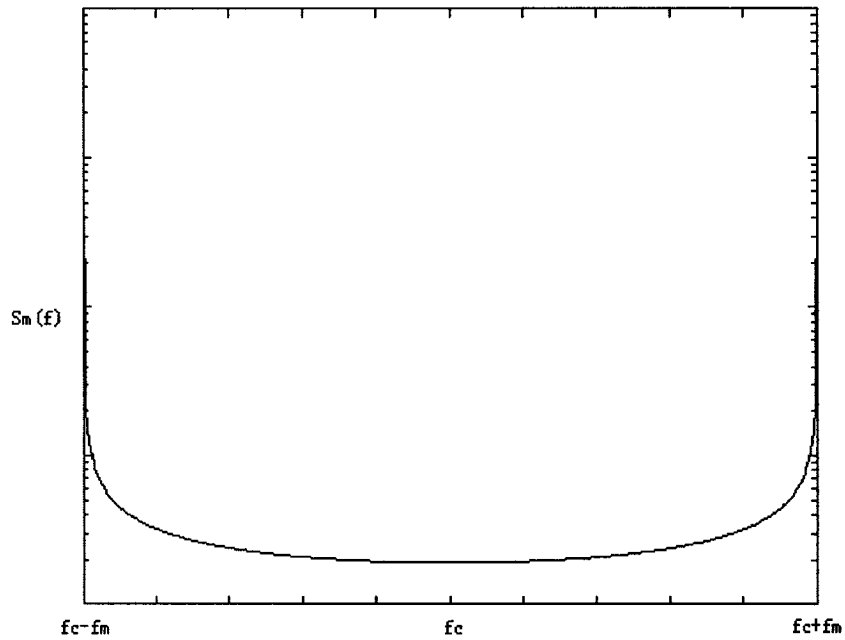

Fig. 2.3 Spectral density of an RF signal with Doppler shift

2.3 Simulation of Multipath Fading Channel

Smith has proposed a simulation method for multipath Rayleigh fading channels [10]. Fig. 2.4 shows this scheme for a pass-band Rayleigh fading channel. This method uses a complex Gaussian random number generator to produce a number of line spectrums in the range of $(f_c - f_m, f_c + f_m)$. Since these line spectrums are symmetric about f_c, only one-half of them, say those in $(f_c, f_c + f_m)$, need to be generated, and the other one-half can be obtained by simply taking the complex conjugate of the generated spectral components. The random valued line spectrum is then multiplied with a discrete frequency representation of $\sqrt{S_m(f)}$ where $S_m(f)$ is given by (2.18). The inverse fast Fourier transform (IFFT) of each complex Gaussian signal represents a purely real

Gaussian random process, which is used to produce the in-phase and the quadrature time-domain signals as represented by $T_c(t)$ and $T_s(t)$, respectively. Then, the in-phase and the quadrature signals are combined according to (2.17) to achieve the amplitude of the Rayleigh fading channel.

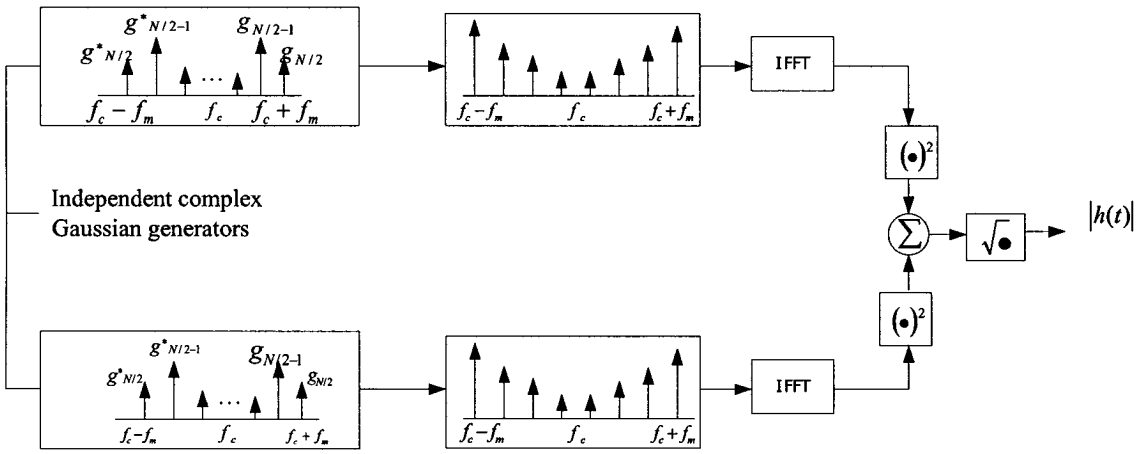

Fig. 2.4 Frequency-domain implementation of pass-band Rayleigh fading

The implementation procedure for the Rayleigh fading simulator can be described as follows.

1. Specify the number of line spectrums, N, used for $\sqrt{S_m(f)}$ and the maximum Doppler frequency shift (f_m). The value for N is usually chosen as a power of two.
2. Compute the frequency spacing between adjacent spectral lines, namely, $\Delta f = 2f_m/(N-1)$. The frequency spacing Δf defines the time duration of the fading signal, i.e., $T = 1/\Delta f$.
3. Generate complex Gaussian random variables for $N/2$ line spectrums in $(f_c, f_c + f_m)$.
4. Obtain the other $N/2$ line spectrums in $(f_c - f_m, f_c)$ by taking the complex

conjugate of those obtained in Step 3.

5. Multiply the in-phase and quadurature frequency components by the corresponding spectrum density $\sqrt{S_m(f)}$.
6. Perform the IFFT on each of the resulting frequency domain I and Q signals and combine the two time-domain quadrature signals to obtain the amplitude of the Ralyleigh fading channel with the associated Doppler shift.
7. Generate a uniformly distributed phase $\phi(t)$ in the interval $[-\pi, \pi]$.
8. Obtain the complete fading channel response by combining the amplitude and the phase.

The above-obtained channel response can be written as

$$h(t) = |h(t)|e^{j\phi(t)} \tag{2.19}$$

which represents a flat Rayleigh fading channel. A frequency selective fading channel comprises several components with variable gains and time delays [1] and therefore, it can be simulated by combing several flat Rayleigh fading channel responses with proper attenuation factors and time delays. This process is shown in Fig. 2.5, where $a_0, a_1, \cdots, a_M$ are the attenuation coefficients associated with the (M+1) paths.

Figs. 2.6 and 2.7 show, respectively, the amplitude and the phase of a Rayleigh fading channel simulated using the above method for the mobile velocity of 60km/h. The simulation results for the Rayleigh fading channel in which the mobile velocity is set to 120km/h and 250km/h are given in Figs.2.8~2.11. It is seen that the channel characteristic changes faster as the mobile's velocity increases. This means that a low-speed mobile

terminal undergoes slow fading and a high-speed mobile terminal suffers from fast fading and more distortion introduced by the channel.

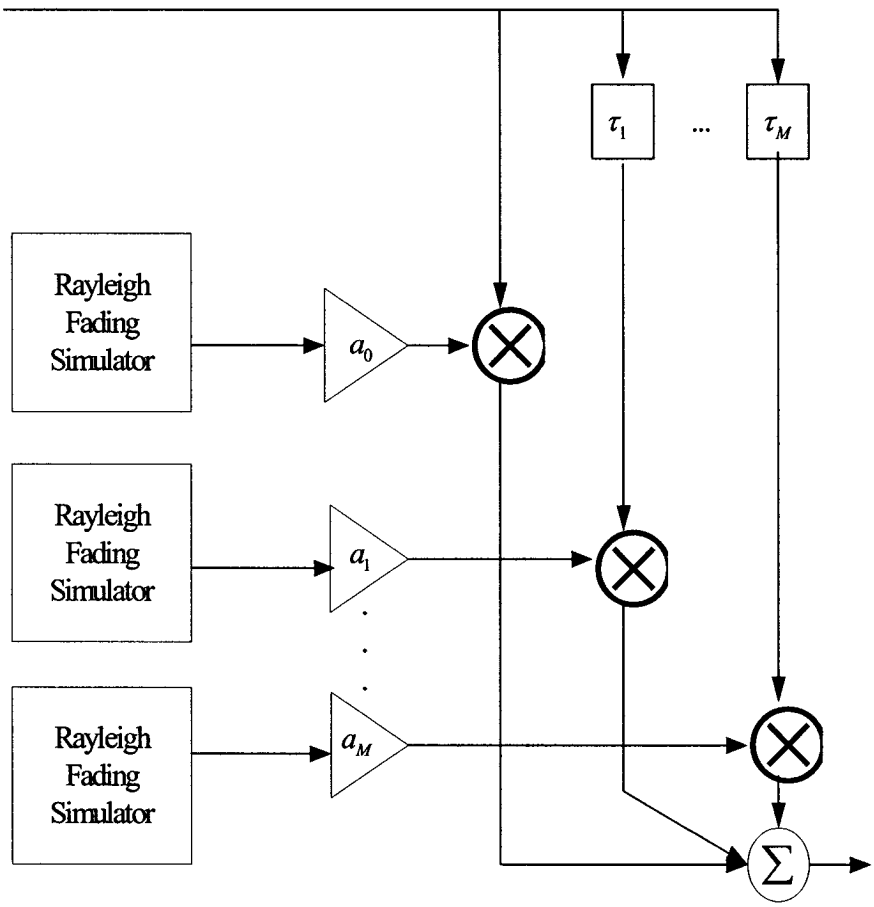

Fig. 2.5 Frequency selective passband Rayleigh fading simulator

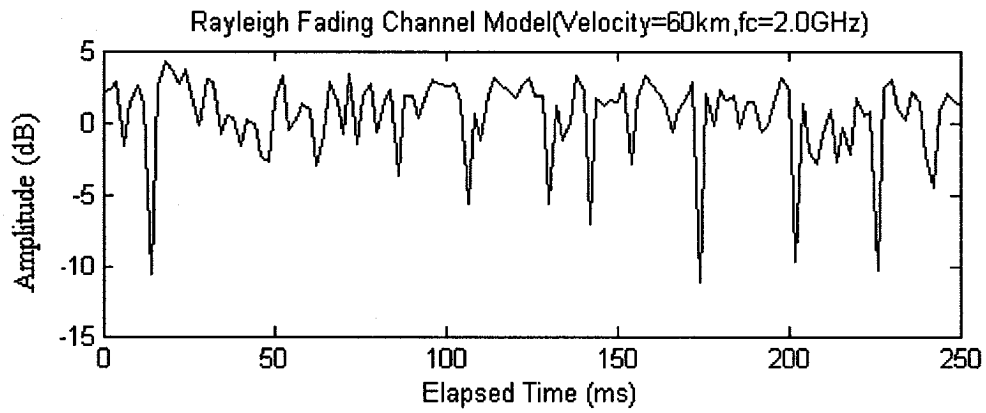

Fig. 2.6 Amplitude of the simulated Rayleigh fading channel (Velocity=60km/h)

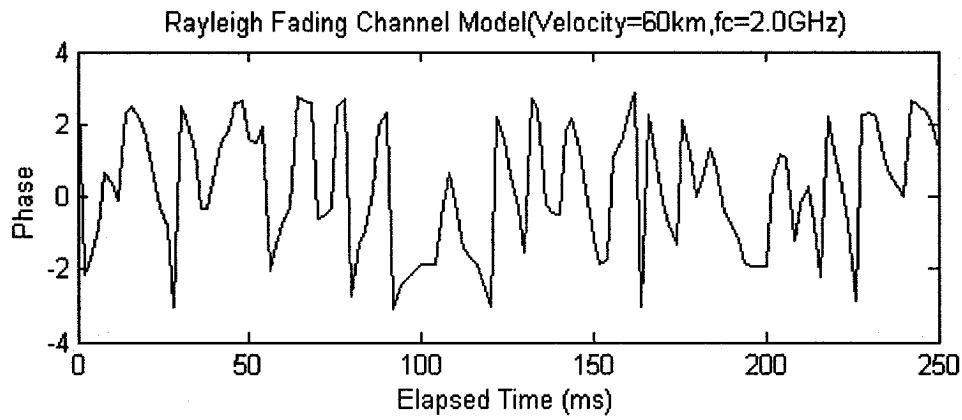

Fig. 2.7 Phase of the simulated Rayleigh fading channel (Velocity=60km/h)

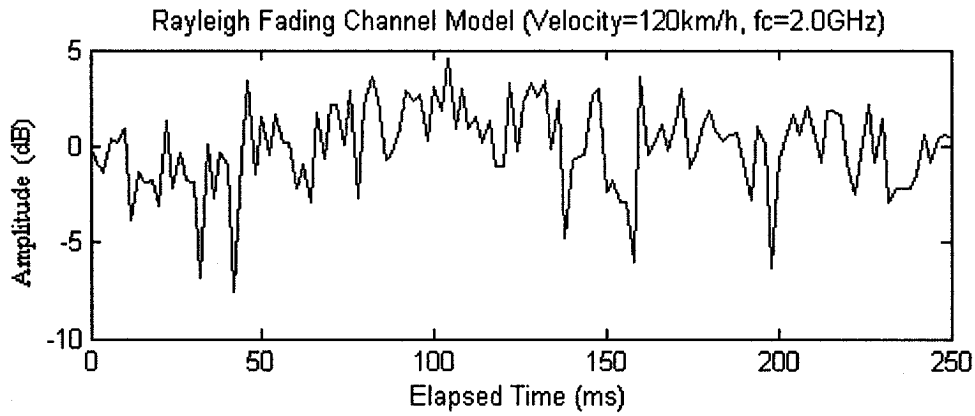

Fig. 2.8 Amplitude of the simulated Rayleigh fading channel (Velocity=120km/h)

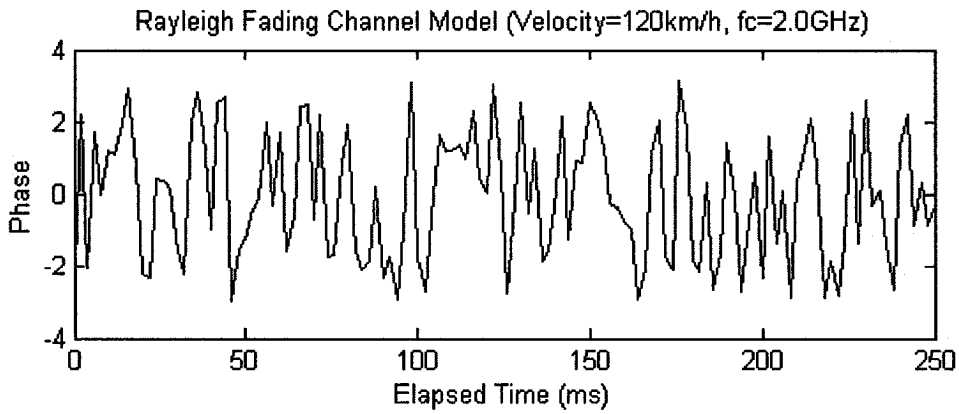

Fig. 2.9 Phase of the simulated Rayleigh fading channel (Velocity=120km/h)

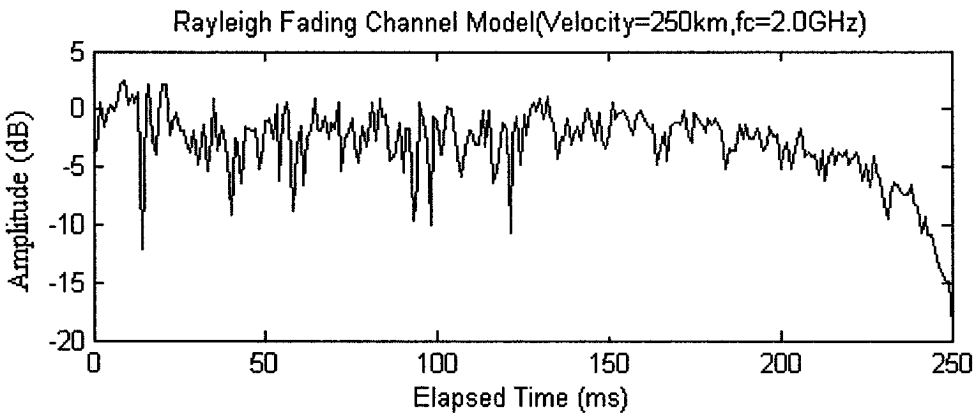

Fig. 2.10 Amplitude of the simulated Rayleigh fading channel (Velocity=250km/h)

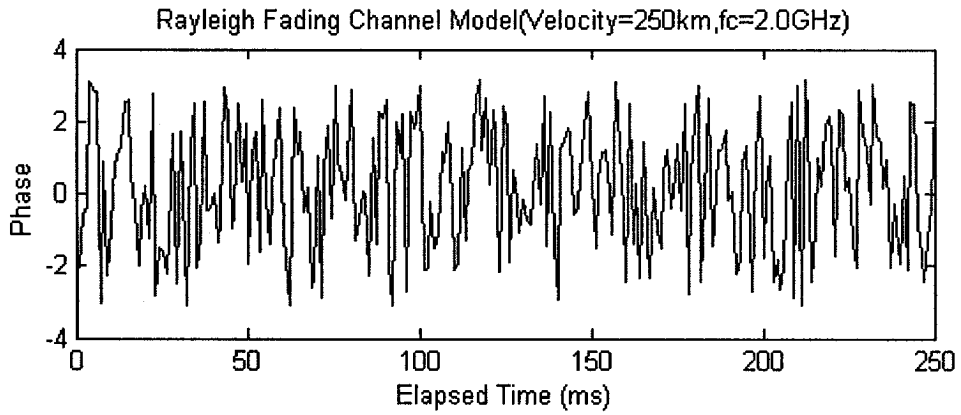

Fig. 2.11 Phase of the simulated Rayleigh fading channel (Velocity=250km/h)

2.4 Conclusion

In this chapter, different wireless mutipath fading channels have been investigated and classified with an emphasis on the mechanism and representation of small-scale fading. In particular, a commonly used fading channel model, i.e., Clarke's model, has been studied, based on which both flat and frequency selective fading channels have been simulated for different mobile velocities. It has been shown through computer

simulations that the fading channel response changes more rapidly as the mobile velocity increases.

Chapter 3

Channel Estimation Techniques and BER Bound

3.1 Introduction

The knowledge of a wireless communication channel is desirable in order to implement optimum reception in the receiver. In reality, however, the true channel information is not available due to its time varying nature. Therefore, a fast and accurate estimation of mobile fading channels is of crucial importance to the system performance. In order to meet the requirement of system performance, the channel response must be estimated as accurate as possible in designing of coherent receivers. Channel estimation in WCDMA systems is to isolate individual multipath components from the received signal and estimate the amplitude and the phase for each of the paths after the transmitted data have been removed.

The 3G standard requires that a coherent Rake receiver be applied in the implementation of WCDMA systems. In both downlink and uplink of WCDMA systems, pilot can be used to facilitate coherent demodulation, making it possible to develop various pilot-assisted channel estimation algorithms. However, the downlink and the uplink have different multiplexing structures and therefore, may require different implementation schemes for channel estimation.

The BER is often used to evaluate communication system performance. A BER bound also provides a guideline for designing communication systems. The commonly used

BER bounds are Chernoff bound and Bhattacharyya bound. The Bhattacharyya bound is more suitable for evaluating the BER performance of digital communication systems [19], [20]. For example, in order to evaluate the effectiveness of a channel estimation algorithm, one can compare the BER performance of the actual system using channel estimation with the Bhattacharyya bound. If the system has a BER curve that is below the Bhattacharyya bound, it is considered acceptable.

This chapter presents an overview of some fundamental channel estimation techniques and a brief discussion of BER performance bounds. As these estimation methods are basically intended for applications in WCDMA systems, the physical channel configurations for both downlink and uplink of WCDMA systems will be first introduced with an emphasis on the dedicated channels which can be used for channel estimation. Then, a few typical channel estimation methods including the maximum-likelihood algorithm, pilot assisted methods etc will be reviewed. The Chernoff and Bhattacharyya bounds will be discussed with some simulation results showing the Bhattacharyya bound for different mobile velocities.

3.2 Brief Description of Dedicated WCDMA Physical Channels

In WCDMA communication systems, various physical channels, each corresponding to a specific spreading sequence or channelization code, are specified for the transmission of different types of information/data including user's data, control information, system configuration etc. The complete WCDMA downlink and uplink physical channels and

their functions are listed in Appendix A. Some of these physical channels are also used for carrying out the signal processing tasks required by the receiver such as system acquisition, synchronization, and channel estimation. For example, in the downlink, both common and dedicated pilot channels provide training symbols for the purpose of channel estimation. In the uplink, only the dedicated pilot channel is available. In this work, we employ dedicated pilot channels for the development of data-aided channel estimation algorithms for WCDMA systems. In the following, we will first describe the structures of the dedicated downlink and uplink physical channels defined in the WCDMA standard.

3.2.1 Dedicated Uplink Physical Channels

Dedicated uplink physical channels consist of layered radio frames. Each frame, lasting 10 ms with a total of 38,400 chips, is divided into 15 time slots, each containing 2,560 chips. The number of bits per slot may vary depending on the data rate in each dedicated physical channel [11]. There are two types of uplink dedicated physical channels, namely, the dedicated physical data channel (uplink DPDCH) and the dedicated physical control channel (uplink DPCCH). In order to avoid magnetic effects for the mobile [7], the DPDCH and the DPCCH are I/Q multiplexed within each radio frame as shown in Fig. 3.1, where A_p and A_d are the gain for the control channel and that for the data channel, respectively. It is noted that by using the multiplexing scheme, the power amplifier efficiency of the transmitter remains the same as the general balanced quadrature phase

shift keying (QPSK) transmission [7].

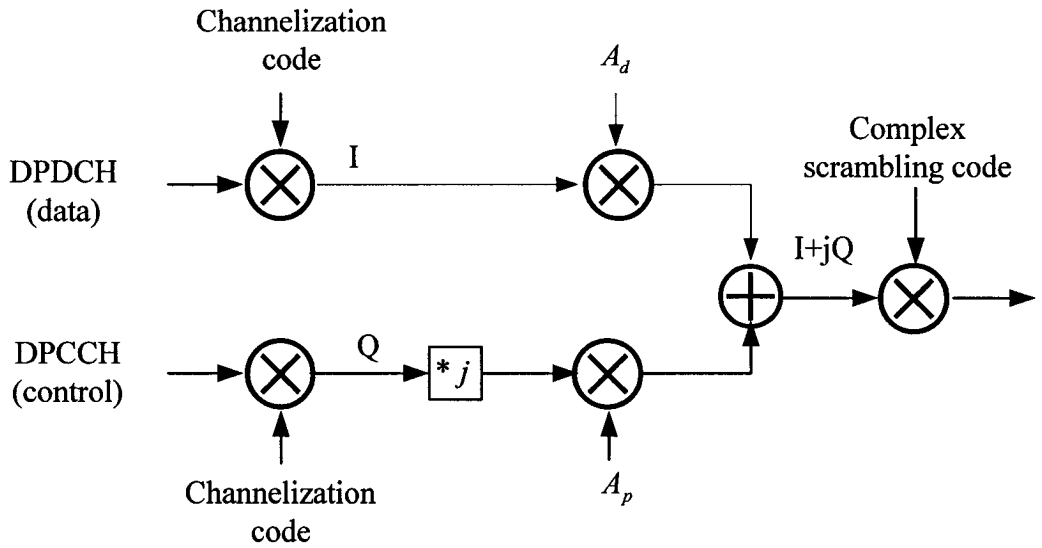

Fig. 3.1 I-Q code multiplexing with complex scrambling

In general, the uplink DPDCH is used to carry user data and the uplink DPCCH is to bear control information including the known pilot for channel estimation in coherent detection, the transmit power control (TPC) command, feedback information (FBI), and an optional transport-format combination indicator (TFCI). Fig. 3.2 shows the frame structure of the uplink dedicated physical channels, where the parameter k indicates the number of bits per slot in the uplink DPDCH and it is related to the spreading factor SF of the DPDCH, i.e., $SF = 256/2^k$. The DPDCH spreading factor may range from 256 to 4. The spreading factor of the uplink DPCCH is always equal to 256, i.e. there are 10 bits per slot in the uplink DPCCH. The number of bits per slot and other fields of the uplink DPCCH $N_{pilot}, N_{TFCI}, N_{FBI}, N_{TPC}$, are listed in Appendix B.

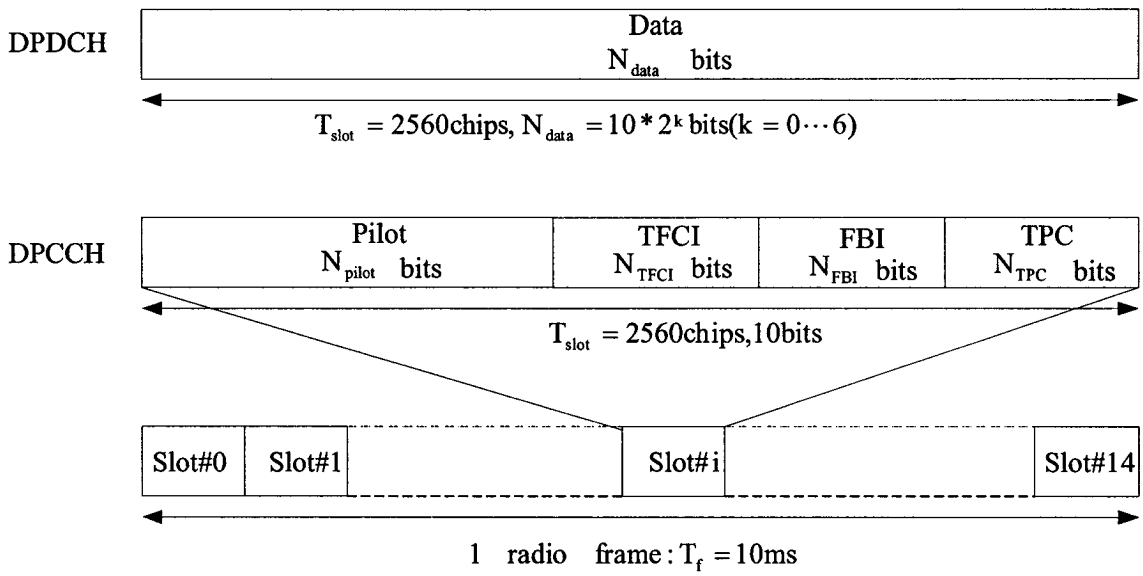

Fig. 3.2 Frame structure of uplink DPDCH/DPCCH

3.2.2 Dedicated Downlink Physical Channels

Unlike the uplink in which several dedicated physical channels are defined, there is only one dedicated physical channel in the downlink, i.e., the downlink dedicated physical channel (downlink DPCH). In the downlink DPCH, user's data are multiplexed with control information. As such, the downlink DPCH can be regarded as a time-multiplexed version of a downlink DPDCH and a downlink DPCCH. Fig. 3.3 shows the frame structure of the downlink dedicated physical channel (DPCH) in which the parameter k denotes the number of bits per slot and it is related to the spreading factor SF of the DPCH by $SF = 512/2^k$. The spreading factor ranges from 512 down to 4. The number of bits per slot and other fields of the downlink DPCH, N_{Pilot}, N_{TPC}, N_{TFCI}, N_{data1}, N_{data2}, is given in Appendix C.

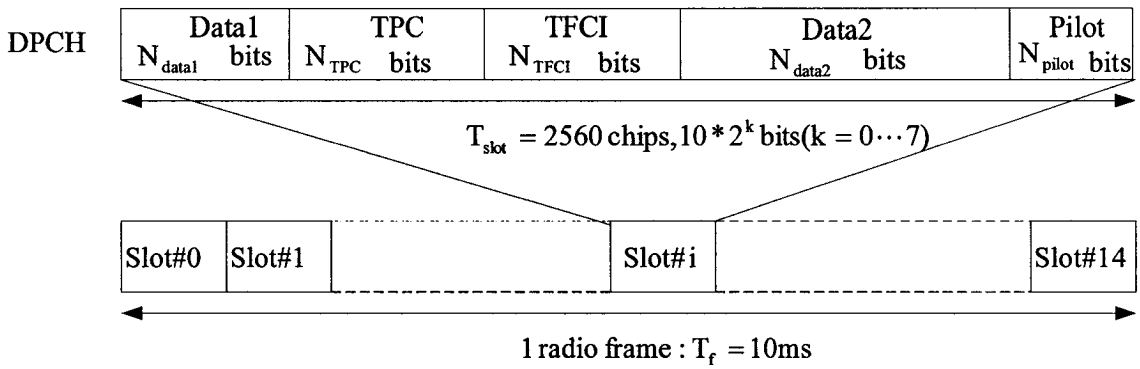

Fig. 3.3 Frame structure of downlink DPCH

3.3 Maximum Likelihood Based Estimation

Maximum-likelihood (ML) estimation is able to provide optimal or nearly optimal performance [12]. As such, it is often used as a basic guideline in developing and evaluating estimation methods for a practical communication system. In general, there are two important ways of estimating unknown parameters in estimation theory, maximum *a posteriori* (MAP) method and the ML approach [12].

The MAP method assumes that the detector maximizes the *a posteriori* probability for all sequences x

$$\hat{x}_{MAP} = \arg\max_{x} p(x \mid r) \tag{3.1}$$

We can use Bayes' rule to rewrite the a posteriori probability as

$$p(x \mid r) = \frac{p(r \mid x)p(x)}{p(r)}. \tag{3.2}$$

On the other hand, the ML procedure can be represented as

$$\hat{x}_{ML} = \arg\max_{x} p(r \mid x) \tag{3.3}$$

From (3.2), the MAP detector needs to know the priori distribution $p(x)$ and the

distribution of r conditioned on the knowledge of the data sequence x. This conditional distribution completely depends on the noise process. Since $p(r)$ does not depend on the data sequence, maximizing $p(x \mid r)$ is the same as maximizing $p(r \mid x)p(x)$. For equally probable data sequences, then maximizing the a posteriori probability is the same as maximizing the likelihood function $p(r \mid x)$, implying that the MAP estimation is identical with the ML method. For WCDMA systems, equal probability of input sequences can always be assumed. Therefore, only the ML based methods are considered. Recent publications [13], [14] have indicated that most of the existing channel estimation algorithms are based the ML estimate principle. For an optimal ML receiver, taking into account the channel response h, maximizing the likelihood function $p(r \mid x,h)$ with respect to (x,h) leads to the following estimate,

$$(\hat{x}_{ML}, \hat{h}) = \arg\max_{x,h} p(r \mid x,h) \tag{3.4}$$

which implies that the receiver performs a joint detection/estimation. A relatively simple solution to the maximization problem (3.4) is to first maximize the joint likelihood function $p(r \mid x,h)$ with respect to h for each possible x and then select the sequence x with the largest likelihood, namely

$$\hat{h}(x) = \arg\max_{h} p(r \mid x,h) \tag{3.5}$$

$$\hat{x} = \arg\max_{x} p(r \mid x, h = \hat{h}(x)) \tag{3.6}$$

The first maximization step yields a conditional channel estimate $\hat{h}(x)$ that is subsequently used in the decision likelihood computation as if it was the true parameter. However, this way may still not be efficient, since each candidate sequence x comes

with its own channel estimate $\hat{h}(x)$ conditioned on that sequence. Many times, channel estimation and data detection are performed separately in the receiver for the convenience of a practical implementation.

There are different approaches of implementing the two disjoint tasks. The first approach is to transmit pilot which is known to the receiver and is used as reference for channel estimation. The second way is to use the decoded data symbols for replacement of the true symbols. Another possible method is to resort to the averaging operation for channel estimation.

In view of the above observations, channel estimation algorithms can be classified into two categories in terms of the algorithm's dependency on training sequence [12].

1. Decision-directed (DD) or data-assisted (DA) method (DD/DA),
2. Non-data-assisted (NDA).

The DA algorithm is able to yield reliable estimation due to the available training sequence that it is known for both the transmitter and the receiver. The bandwidth efficiency is more or less affected by the overhead of training sequence/data. In this thesis, pilot is used as the known training data, thus we also call DA as pilot-assisted (PA) algorithm.

When the detected sequence is used as if it was the actual sequence, DD channel estimation algorithms are applied. Its performance can approach that of DA, especially in the case of high SNR. However, a DD algorithm may produce decision errors. In order to eliminate the decision errors, DD algorithms should be aided by other reliable

information.

NDA algorithms can usually be implemented by averaging the received signals in order to remove the data dependence. It is limited to some specific transmission format, and turns out to cause performance degradation because of the lack of the reliable training data, especially at a low SNR level.

Pilot symbols are already specified in WCDMA standards so that they are always available to be used as reference for channel estimation. Therefore, pilot-assisted algorithms become the first consideration in designing the WCDMA receiver with channel estimation. Different pilot patterns can be adopted to satisfy the system requirement. In order to improve the transmission efficiency, the pilot should be as short as possible provided that the BER performance satisfies the system requirement. The common pilot can be used in the design of PA channel estimation algorithms for a WCDMA communication system [49], [50]. Note that such a scheme is only suitable for the downlink since common pilot is not available in the uplink. The other choice of reference symbols for PA algorithms is to employ the pilot carried in the dedicated physical channels. In this aspect, a number of schemes have been proposed for both downlink and uplink [23]~[25] [38], [40]~[42]. Sine the only difference between the downlink and the uplink is that the multiplexing mode of the pilot, the PA algorithm proposed for downlink is also suitable for the uplink as long as some minor modifications to the receiver structure are made. In [40, 41], the estimated channel response is obtained based on linear interpolation. In [38] and [42], the estimated channel response is obtained

by extending the observation period to more than one slot and making use of pilot belonging to two slots or more. Though the estimation accuracy and system performance may vary from one method to another, most of these methods are only suitable in slow fading environments. As the fading becomes faster, the estimation error becomes larger and consequently the system BER performance gets worse. Therefore, PA algorithms cannot provide satisfactory estimation accuracy in fast fading channels.

Compared with PA algorithms, the superior tracking capability of DD algorithms makes it is more suitable to estimate fast-fading channels. A DD channel estimation approach for Rake receiver has been suggested in [22]. This approach achieves a considerable performance gain in multipath fast fading environments. However, in this method it is assumed that correct data decisions are made, i.e., no decision error occurs in the receiver. This assumption is not true for a practical communication system. Therefore, this approach is only used for theoretical analysis. As a matter of fact, DD algorithms are rarely used alone due to the decision error problem.

A combined symbol-aided and decision-directed (SADA) channel estimation method has been proposed for the estimation of mobile satellite fading channels [36]. This technique has been extended as a joint PA and DD scheme for applications in WCDMA communication systems [37]. This PADD scheme can provide reliable and accurate estimation for fast fading channels. However, it is not practically feasible, since it uses a moving average filter whose length should vary depending on the channel condition.

3.4 BER Performance Bound for WCDMA Systems

Channel estimation is important for a coherent receiver and the quality of channel estimation (QCE) is one of the main factors which affect the system performance. We can use the system BER performance to investigate QCE for different channel estimation schemes, a better BER performance should correspond a better channel estimation result or higher QCE. The BER performance upper bound is a theoretical guideline in designing a communication system, that is, only those schemes which achieve better BER performances than the upper bound can be accepted. Concerning channel estimation, the BER performance with a channel estimate should be better than the BER upper bound with the same channel estimate. In the following, the upper bound of BER performance in terms of QCE will be addressed.

3.4.1 Channel Estimation Quality

QCE is used to measure the accuracy of a channel estimation result. In [13], QCE is defined as the ratio of the mean square value of the true channel response to the mean square value of the channel estimation error. Considering an unbiased channel estimate $\hat{h}(n)$ of true channel response $h(n)$ that can be expressed as

$$\hat{h}(n) = h(n) + v_e(n) \tag{3.7}$$

where $v_e(n)$ is the estimation error, the QCE ς is defined as

$$\varsigma = E\left[|h(n)|^2\right] \Big/ E\left[|v_e(n)|^2\right] \tag{3.8}$$

A low-pass filter is often used in the receiver to remove the additive noise in order to obtain an accurate channel estimation result. Since the Doppler spectrum is usually not known or may change with time, our best knowledge about the channel response $h(n)$ is a random process with a maximum Doppler frequency f_m. Therefore, a low-pass filter with cut-off frequency equal to f_m can be used in the estimation process.

The close-form representation of QCE for PA algorithms can be derived from theoretical analysis. For DD algorithms, it is difficult to derive such a formula due to the decision symbol errors. Therefore, the following analysis focuses on PA algorithms for WCDMA communication systems.

In WCDMA systems, when the code-division multiplexed (CDM) pilots are used to establish references for performing channel estimation in the uplink, we denote the data to pilot power ratio, i.e., the ratio of the user's data power to the CDM pilot power, as P. Alternatively, for the downlink, as time-division multiplexed (TDM) pilot is used as reference in the channel estimation, we denote the pilot insertion ratio, i.e., the ratio of the average number of data symbols to the average number of pilot symbols, as M.

When the estimated channel response is obtained by passing the unfiltered channel response through a low-pass filter in either downlink or uplink, the channel estimation quality QCE ζ of the downlink or uplink can be expressed as [13]

$$\zeta_d = f_{cp}\gamma_c /(2f_m(M+1)) \tag{3.9}$$

or

$$\varsigma_u = f_{cp}\gamma_c /(2f_m(P+1)) \tag{3.10}$$

where

ς_d: the QCE of downlink,

ς_u: the QCE of uplink,

f_{cp}: pilot chip rate,

γ_c: chip level SNR.

Comparing (3.9) and (3.10), we can find that the channel estimator in the case of TDM and that of CDM are equivalent in terms of the channel estimation quality QCEζ, provided that they have the same pilot chip rate f_{cp} and the same chip SNR γ_c and satisfy $P = M$.

3.4.2 BER Performance Bound

It has been further shown in [13] that the system BER performances are also equivalent when TDM and CDM pilot are employed for channel estimation when the QCE of downlink and uplink are equivalent. Therefore, we will not distinguish TDM and CDM schemes in our analysis. In what follows, a BER bound, namely, the Bhattacharyya bound, will be used as the upper bound in WCDMA communication systems when PA channel estimation algorithms are applied.

As we have mentioned, the Bhattacharyya bound is particularly suitable for a digital communication system which employs a ML algorithm in the receiver [19]. The Bhattacharyya bound can be derived from the Chernoff bound for a digital

communication system. The Chernoff bound can be expressed as [20]

$$P_r(x > X) < \underset{\rho>0}{Min} e^{?X} E(e^{?x}) \tag{3.11}$$

where

x: random variable,

X: known value,

ρ: positive constant.

When the random variable represents a likelihood function and $X = 0$ so that the probability (3.11) becomes an error probability, applying the Chernoff bound gives rise to the Bhattacharyya bound as given by [20]

$$D_B \le \int_{-\infty}^{\infty} \sqrt{p_0(x) p_1(x)} dx \tag{3.12}$$

where $p_0(x)$ and $p_1(x)$ are, respectively, the probabilities that "0" and "1" are sent from the transmitter. The Bhattacharyya bound has been applied to the analysis of BER performance for WCDMA communication systems in [13]. For pilot-assisted channel estimation, the Bhattacharyya bound can be expressed in terms of the SNR γ_c and the QCE ς (ς_u or ς_d) as given by

$$D_B = \frac{1}{(1+\gamma_c)\left(1-\frac{\gamma_c}{1+\varsigma+\gamma_c}\right)} \tag{3.13}$$

The Bhattacharyya bound of the coherent receiver for a Rayleigh fading channel with the known channel response $h(n)$ can be written as [21]

$$D_B = \frac{1}{1+\gamma_c} \tag{3.14}$$

Comparing (3.13) with (3.14), we can see that there is always a performance loss when using the estimated channel response instead of the true one.

Fig. 3.4 shows Bhattacharyya bounds of the BER performance for different mobile velocities and the true channel. In this simulation, we have assumed that the carrier frequency is 2.14Ghz, the number of pilot symbols per slot is set to be 8, and the velocities of a mobile terminal is set to 60km/h, 120km/h and 250km/h. It is seen that the Bhattacharyya bound increases with the increase of the mobile velocity. This indicates that for the same channel estimation scheme, the system BER performance in a slow fading channel is always better than that in a fast fading channel.

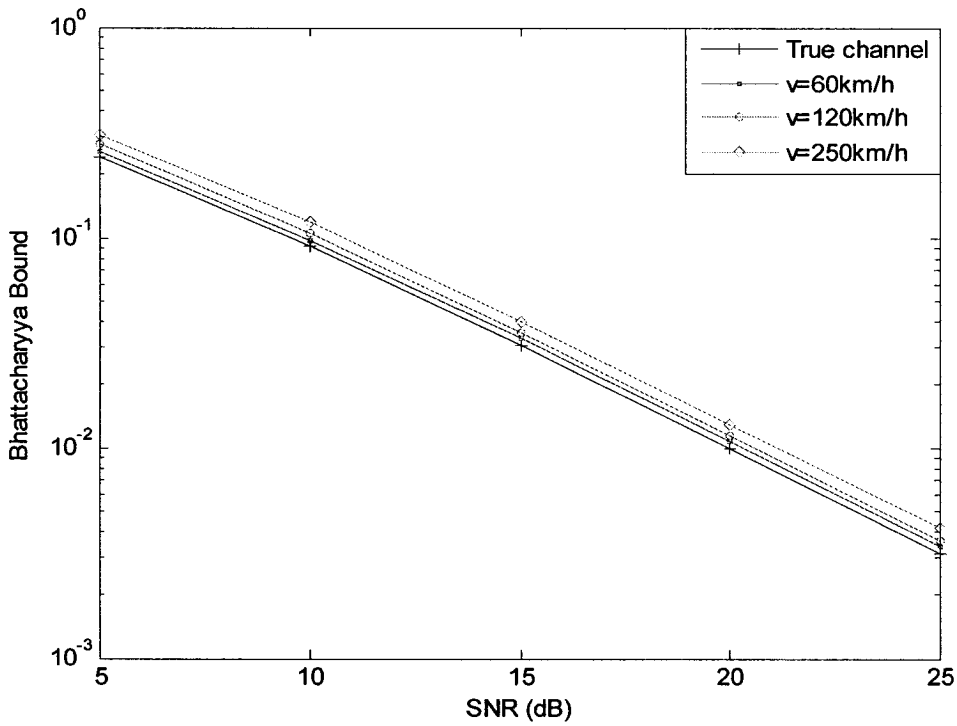

Fig. 3.4 Bhattacharyya bounds for different mobile velocities

3.5 Conclusion

In order to develop pilot/data aided channel estimation techniques for WCDMA systems, the physical channel configurations for both downlink and uplink of WCDMA systems have been reviewed, showing the frame and slot structures as well as multiplexing schemes for both links. Some of the ML based estimation approaches reported in literature have been discussed and divided into two categories, i.e., data aided and non-data aided techniques, pointing out that the performance of a channel estimation method mainly depends on the mobile's velocity. The Bhattacharyya bound of the BER performance has also been reviewed and simulated for different mobile velocities, showing its importance as a reference in evaluating the performance of a channel estimation technique.

Chapter 4

Pilot-Assisted and Decision-Directed Channel Estimation

4.1 Introduction

In the last chapter, we have stated that both pilot and decision symbols can be used as reference for WCDMA channel estimation. The pilot-assisted algorithms are reliable and accurate for the estimation of slow-fading channels [12]. For fast fading channels, however, they cannot track the channel very well and hence cannot provide good channel estimation. Decision-directed estimation algorithms, while being able to track the fast change of a fading channel, usually suffer from decision symbols error problem and even cause the hang-up in some situations [12]. Moreover, conventional decision-directed amplitude and phase tracking techniques are prone to false lock and therefore, cannot guarantee satisfactory estimation performance. One possible solution is to combine these two techniques to constitute a two-stage estimation scheme, which makes use of the good reliability of the pilot-assisted algorithm and the fast tracking property of the decision-directed one in order to implement a robust and accurate estimation technique for fast fading channels.

In this chapter, we propose a two-stage pilot-assisted (PA) and decision-directed (PADD) WMSA channel estimation technique for WCDMA systems. The first stage is to implement an initial channel estimation using the pilot symbols along with the WMSA

method. The second stage is to perform a fine estimation by taking into account the information of the fading channel that is extracted from the received data symbols. The proposed method will be simulated for both downlink and uplink of WCDMA systems and will be compared with some of the existing methods.

4.2 Proposed Pilot-Assisted and Decision-Directed Channel Estimation

Fig. 4.1 and Fig. 4.2 show block diagrams of a coherent Rake receiver with a channel estimation filter for WCDMA downlink and uplink, respectively. The structures of the downlink and uplink receivers are very similar except that different spreading sequences are used. In the downlink, one spreading sequence is utilized to despread the received QPSK symbols and the resulting despread symbols are further partitioned into data symbols and pilot symbols. In the uplink, two orthogonal spreading sequences corresponding to hard decision symbols and pilot symbols, respectively, are employed to obtain the I and Q symbols. Note that the implementation of the channel estimation filter is the same for both links, although the sources of pilot symbols are different. As such, in this section, we concentrate our discussions on the downlink only. A simulation study of the proposed estimation method for both downlink and uplink will be carried out in the next section.

4.2.1 WMSA Channel Estimation Technique

In WCDMA communication systems, the time division multiplexed pilot is used for the

downlink and the code division multiplexed pilot for the uplink. Based on the TDM and the code division multiplexing CDM structures, a weighted multi-slot averaging (WMSA) channel estimation method performs a weighted average of the data over an observation period of multiple slots, in which each slot uses the same weight [38]. For the downlink, the received multipath signal is despread by a matched filter and then split into L QPSK signals that correspond to different paths with different time delays. The matched filter is equivalent to a bank of synchronous correlators, each realized by integrating over one symbol period T_s, the product of the received signal and the spreading waveform regenerated at the receiver and synchronized to the time delay of each path. Let us denote the received signal as $r(t)$. It can be expressed as

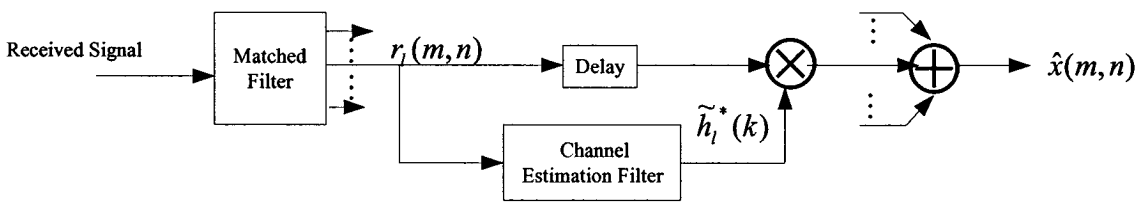

Fig. 4.1 Rake receiver with channel estimation filter for downlink

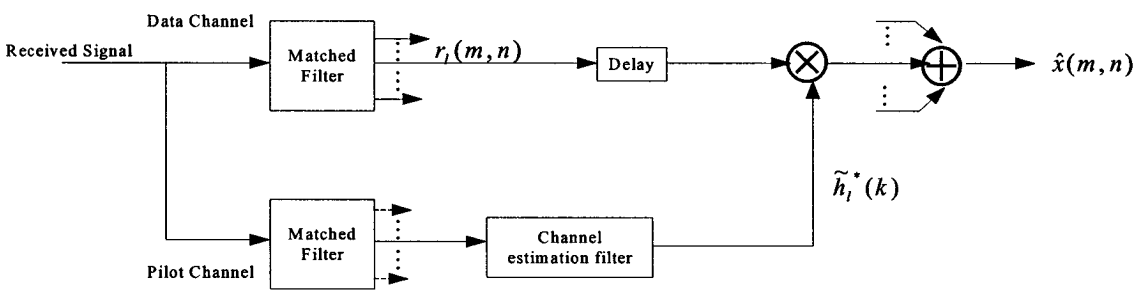

Fig. 4.2 Rake receiver with channel estimation filter for uplink

$$r(t) = \sum_{l=0}^{L-1} r_l(t) = \sqrt{2S} \sum_{l=0}^{L-1} h_l(t) s(t - \tau_l) + n(t) \tag{4.1}$$

where

$r(t)$, received signal at the receiver,

$r_l(t)$, received l^{th} path signal,

S, average power of the received signal,

$h_l(t)$, complex channel impulse response of the l^{th} path,

τ_l, l^{th} path delay,

$s(t)$, modulated data waveform.

In order to perform coherent demodulation, the WMSA channel estimation filter is first used to obtain the estimate of the channel impulse response, that is, for the m^{th} symbol of n^{th} slot, $\tilde{h}_l(m,n) = \sqrt{2S} h_l(m,n)$ for the l^{th} path. The output of the matched filter, $r_l(m,n)$, is then multiplied by the complex conjugate of the corresponding channel estimate $\tilde{h}_l(m,n)$, and combined with the counterparts from other paths. Thus, the output signal at the m^{th} symbol in the n^{th} slot of the coherent Rake combiner can be written as

$$\hat{x}(m,n) = \sum_{l=0}^{L-1} r_l(m,n) \tilde{h}_l^*(m,n), \; (m = N_P, N_P + 1, \cdots, N_P + N_D - 1) \tag{4.2}$$

where N_P and N_D represent the number of pilot symbols and that of data symbols in each time slot, respectively. Fig. 4.3 shows a detailed block diagram of the WMSA channel estimation method. It consists of three filters $H_1(f), H_2(f)$ and $H_3(f)$. The first filter $H_1(f)$ serves as an integrator that performs integration over N_P-pilot

symbol periods. The second filter $H_2(f)$ is a 2K-tap transversal filter with tap coefficients $\alpha_0, \alpha_1, \ldots, \alpha_{K-1}$, often called channel estimation filter. The third one $H_3(f)$ is equivalent to a T_{slot}-second hold circuit.

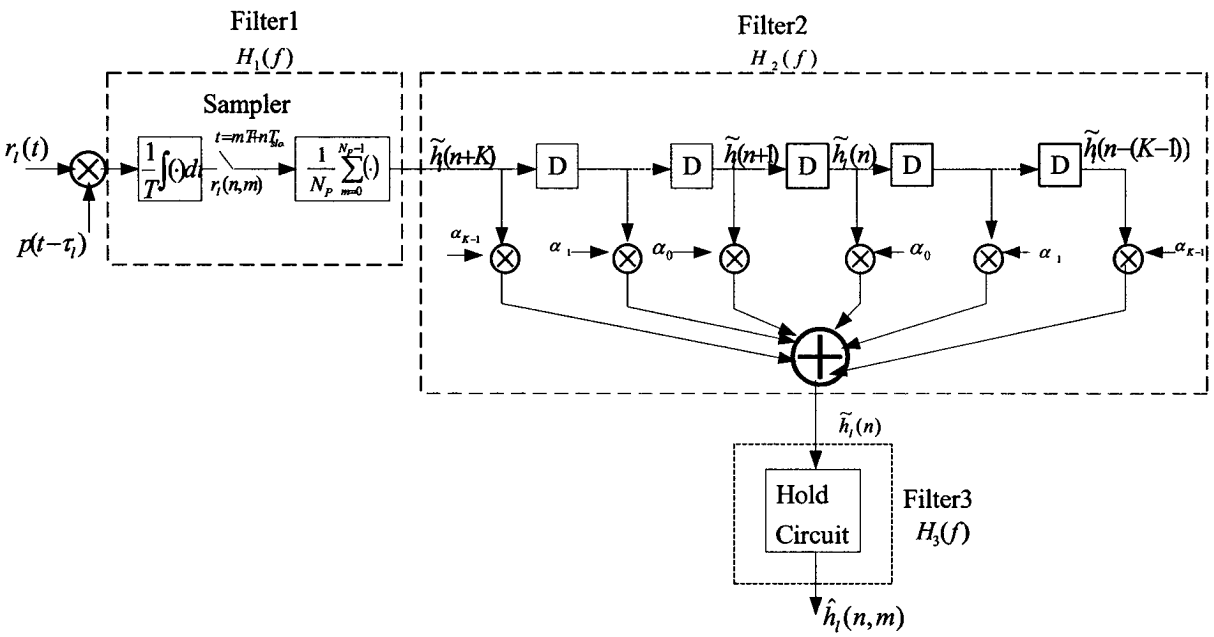

Fig. 4.3 WMSA channel estimation filter ($D = T_{slot}$)

First, the instantaneous channel estimation is performed by using N_P pilot symbols belonging to the n^{th} slot, that is,

$$\tilde{h}_l(n) = \frac{1}{N_P}\sum_{m=0}^{N_P-1} r_l(m,n)x_P^*(m,n) \tag{4.3}$$

As the fading variation during N_P pilot symbols can be neglected, $\tilde{h}_l(n)$ can be approximately given by $\tilde{h}_l(n) \approx \sqrt{2S}\tilde{h}_l(m=0,n) + n_l(n)$, where $n_l(n)$ is a complex-valued Gaussian noise with a variance of $(N_0/T)/N_P$. Thus, the SNR of the channel estimate

has increased N_P times per symbol relative to the SNR of the received signal. In the case of slow fading, since the channel gain remains almost the same over a period of several slots, a number of consecutive channel estimates can be combined in order to achieve a smoothed version of the channel estimate. Therefore, the WMSA method spans 2K slots and yields a channel estimate as given by

$$\hat{h}_l(n) = \sum_{i=0}^{K-1} \alpha_i \tilde{h}_l(n-i) + \sum_{i=1}^{K} \alpha_{i-1} \tilde{h}_l(n+i) \tag{4.4}$$

where $\hat{h}_l(n)$ denotes the channel estimate for l^{th} slot.

By choosing appropriate weighting factors α_i's, it is possible to implement an accurate channel estimation for slow fading environments where a large number of pilot symbols across multiple slots are available. It has been known that in the case of very slow fading, the 2K-tap WMSA channel estimation filter is able to increase the SNR of the channel estimate by a factor of $N_p\left(\sum_{i=0}^{K-1}\alpha_i\right)^2 \Big/ \sum_{i=0}^{K-1}\alpha_i^2$ [38]. However, as fading becomes faster, the estimation filter tends to fail to track the channel characteristic.

It has been shown in [38] that the WMSA method works well for the 3rd generation WCDMA communication systems when the Doppler frequency is below 185 Hz, which is translated to a mobile speed of less than 100 km/h at the 2 GHz frequency band. The WMSA approach simply considers the channel gain to be a constant over a period of one or more slots. However, this is not true in real fading scenarios, especially for high-speed receivers. With the increase of the mobile velocity, the WMSA estimator cannot track the channel perfectly. The reason is that the pilot-assisted WMSA method has not exploited

the information of the received data symbols.

4.2.2 Proposed Channel Estimation Method

As we have described in Chapter 3, there are basically two classes of data-aided channel estimation methods for WCDMA systems, namely, the pilot-assisted method and the decision-directed method. The pilot-assisted approach is more suitable for slow-fading channels. For fast-fading channels, a pilot-assisted estimator may not be able to learn the channel response as rapidly as the channel varies. In order to obtain a good estimation performance, more reference symbols are needed in the estimation process. The first possible solution is that one can increase the number of pilot symbols in each time slot. However, this degrades the transmission efficiency of the system and cannot satisfy the requirements of the system design. Therefore, this method is not always preferred from the system design point of view. Alternatively, we can make use of data symbols as they also carry the channel information. Therefore, decision-directed algorithms have been proposed for channel estimation, in which a hard decision of data symbols needs to be made. Note that there might be decision errors which would affect the channel estimation accuracy. In particular, when the SNR is low, the estimation result will not be accurate, if only data symbols are used, due to a possible large number of decision symbol errors. The advantage of a decision-directed algorithm is its fast tracking capability in the estimation of fast fading channels. In order to overcome the problem caused by decision errors, one can use more reliable pilot symbols to improve the estimation accuracy. Based

on this idea, we propose a pilot-assisted and decision-directed (PADD-WMSA) method that combines the pilot-assisted and the decision-directed algorithms. Fig. 4.4 shows the diagram of the proposed two-stage scheme.

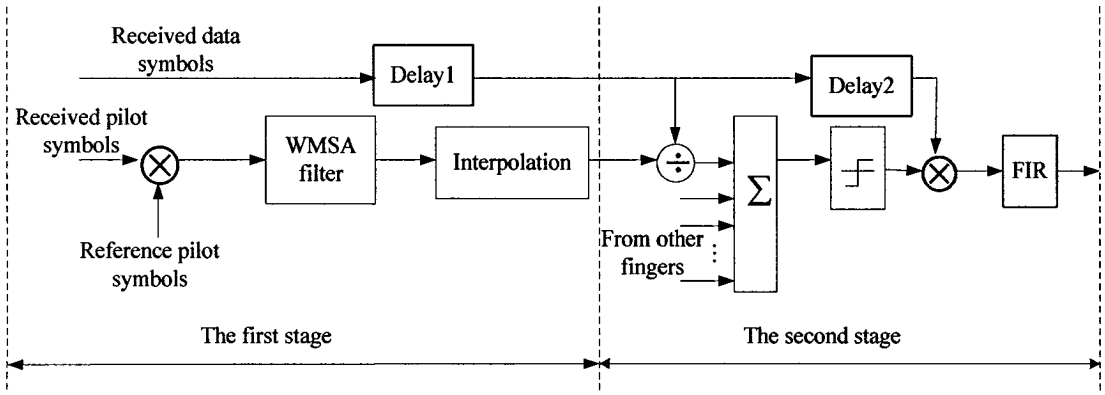

Fig. 4.4 Proposed pilot-assisted and decision-directed channel estimation

In the first stage, the pilot symbol-based WMSA channel estimation filter is employed to obtain a coarse estimate for one slot of the fast-fading channel. Then, a linear interpolation scheme is employed to obtain the estimate for each symbol. The second stage is to carry out a fine estimation via the channel information extracted from the decision data symbols. As shown in the figure, the received data symbols are delayed and divided by the complex channel gain obtained in the first stage in order to get rid of the distortion incurred in the received data. The corrected data obtained in all fingers of the Rake are combined using the maximal-ratio combining algorithm [1], and then sent to the decision unit for hard decision. Then, an improved channel estimate can be achieved by using the hard-decision symbols in conjunction with the further delayed version of the received data. Finally, the channel estimate thus obtained is further filtered for the best estimation result. The low-pass FIR filter in the second stage is mainly used to reduce the

noise from the estimated channel response. The proposed estimation procedure for the downlink channel can be summarized as follows.

1. For each finger, obtain a coarse channel estimate for each slot by using the WMSA channel estimation method along with the received pilot symbols.
2. Use a linear interpolation scheme to obtain an estimate of the complex channel gain for each symbol.
3. Divide the received data symbols by the corresponding complex channel gain obtained in Step 2.
4. Combine the clean data from all the fingers and make a hard decision for the combined data symbols.
5. Divide the received and delayed symbols by the decision symbols obtained in Step 4 to get an improved complex channel gain.
6. Further filter the above-obtained complex channel gain to achieve a fine channel estimate.

In Step 5, the complex division can be replaced by complex conjugate operation, since the QPSK modulation is used in downlink WCDMA communication systems. The estimation procedure for uplink is similar to the downlink, except that in Step 1, the CDM pilot symbols instead of TDM ones are used for coarse channel estimation.

4.3 Computer Simulation of the Proposed Method

In this section, we will show through computer simulation the performance of the

proposed PADD-WMSA channel estimation method for both downlink and uplink WCDMA systems. Both the amplitude and the phase of the estimated channel as well as the BER performance of the WCDMA systems, resulting from the proposed method, will be shown along with that obtained from the basic WMSA estimator. The Bhattacharyya bound will also be plotted for comparison.

4.3.1 Simulation for WCDMA Downlink

Table 4.1 shows relevant parameters and assumptions that are used for the modelling and simulation of the downlink WCDMA system. All of these parameters are specified in the WCDMA standard [11], [35]. The channel is assumed to be multipath Rayleigh fading channel. The Doppler frequency can be determined according to the mobile velocity [1]. In our simulation, we have used four (K=2) slots of pilot symbols for the initial channel estimation. The weighting coefficients of the WMSA filter are obtained through computer simulation [38]. It is assumed that the three paths have equal energy, i.e., the impulse responses of the three paths have identical variance, and the maximum ratio combining algorithm is used in the Rake receiver. The FIR filter in the second stage is a 13^{th} order low-pass filter designed by using the Kaiser Window method, its cut-off frequency being determined according to the velocity of the mobile receiver. For low-speed receivers, the cut-off frequency can be set relatively small in order to remove as much noise as possible while the channel energy is not considerably affected. For high-speed receivers, however, one has to set a large cut-off frequency since the channel is spread in a large frequency

range. It should be mentioned that a low-pass filter with a large cut-off frequency can accommodate more noise, leading to a less accurate estimation result.

Table 4.1 Parameters and assumptions for downlink system simulation

Number	Description	Parameter
1	Spreading code	OVSF
2	Spreading factor	128
3	Data modulation	QPSK
4	Chip rate	3.84 Mchips/s
5	No. of Multi-paths	3
6	No. of fingers	3
7	Synchronization	Perfect
8	Path-delay	Known
9	Slot format	11
10	Channel model	Rayleigh+Gaussian
11	Mobile velocity	60km/h,120km/h,250km/h
12	Number of users	1
13	Carrier frequency	2.14 GHz
14	WMSA Weights	$\alpha_0 = 1.0, \alpha_1 = 0.6$

The estimated channel amplitude and phase for one path are shown in Figs. 4.5 and 4.6, and the BER plot of the system is given in Fig. 4.7, where the mobile velocity is set to 60 km/h and the SNR to 10dB. In these figures, we have also shown the true channel characteristic along with the estimation results given by the WMSA method for comparison. The simulation results with respect to the mobile velocity of 120km/h and that of 250km/h are shown in Figs. 4.8~4.10 and Fig. 4.11~4.13, respectively. Table 4.2 lists some of the BER values for the downlink system. From these simulation results, the following observations can be made.

1. The proposed PADD-WMSA scheme outperforms the WMSA method for all the three mobile velocities 60km/h, 120km/h and 250km/h. The estimation result of the

proposed method is close to the true channel case.

2. Both the WMSA method and the proposed PADD-WMSA scheme work well for slow fading channels. This can be seen from the simulation results shown in Figs. 4.5~4.7 when the mobile velocity is 60km/h, in which the estimation errors for the channel amplitude and phase given by the two methods are comparable and relatively small. The BER performances obtained from the two algorithms are also close to that for the true channel case. This can be seen from the BER data in Table 4.2. For instance, the BER values for WMSA, PADD-WMSA and the true channel are 0.0746, 0.0566, and 0.0532, respectively, at the SNR level of 10 dB, indicating that both the WMSA and the PADD-WMSA can track the channel well and can perform an accurate estimation.
3. With the increase of the receiver's speed, the estimation errors both in the channel amplitude and in the phase given by the two methods become larger and the system BER performance degrades slightly as well. However, the proposed method exhibits a smaller estimation error in comparison to the WMSA method. For a very high speed, such as 250km/h, the BER performance using the WMSA method appears unacceptable as seen from Fig. 4.13 where some BER values even exceed the Bhattacharyya bound. However, the proposed scheme is able to estimate the channel characteristic with a good precision and the BER performance is much better than that using the WMSA method. Therefore, the proposed method is capable of working in both slow and fast fading environments.

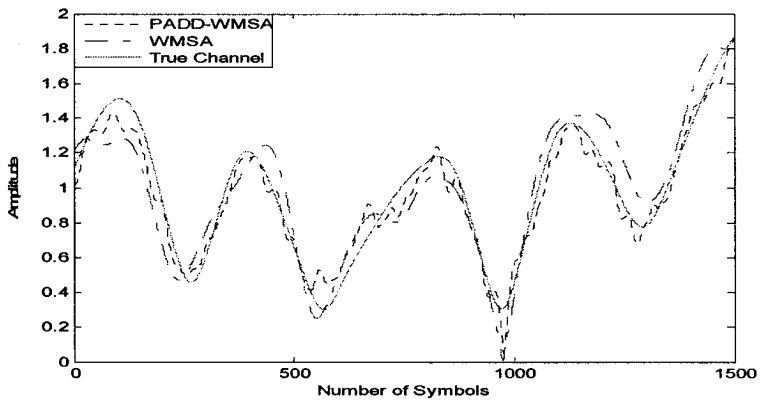

Fig. 4.5 Estimate of downlink channel amplitude (Velocity=60km/h, SNR=10dB)

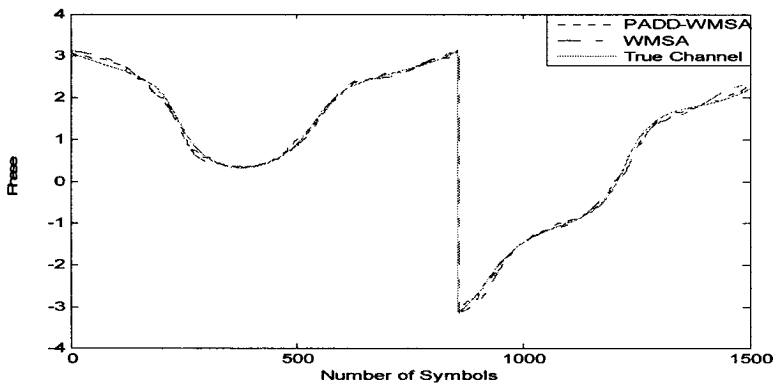

Fig. 4.6 Estimate of downlink channel phase (Velocity=60km/h, SNR=10dB)

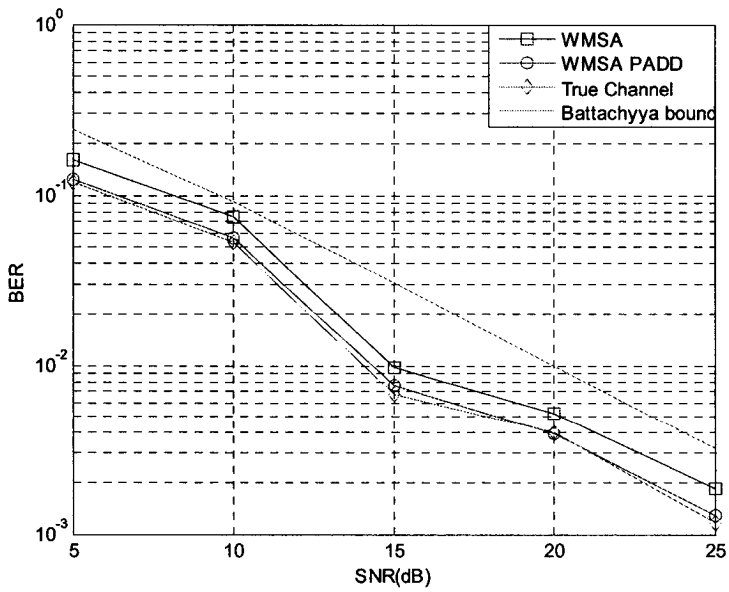

Fig. 4.7 BER performance of downlink (Velocity=60km/h)

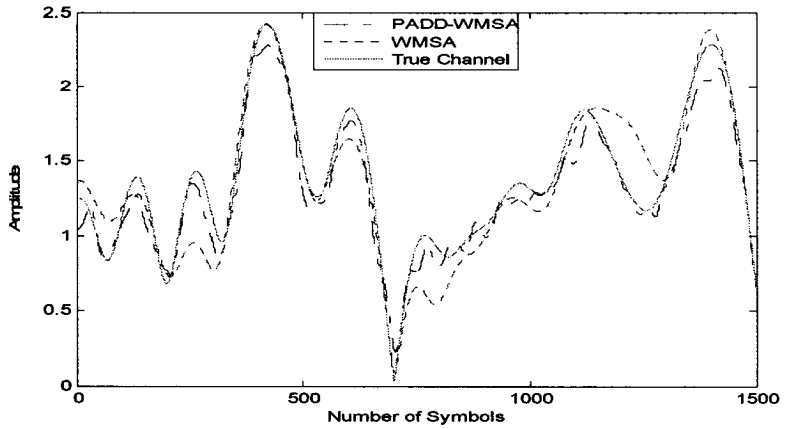

Fig. 4.8 Estimate of downlink channel amplitude (Velocity=120km/h, SNR=10dB)

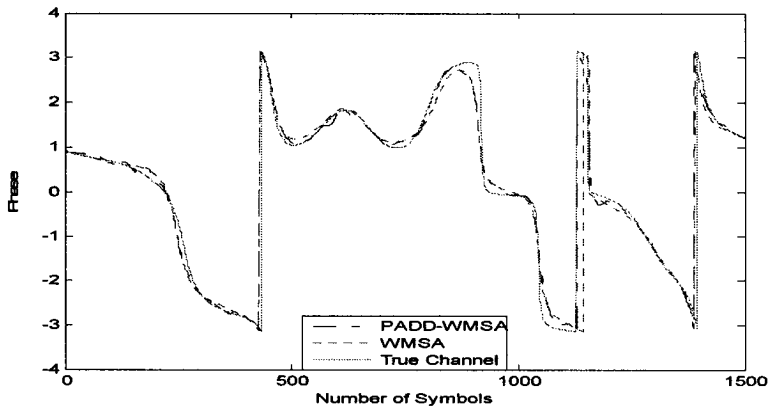

Fig. 4.9 Estimate of downlink channel phase (Velocity=120km/h, SNR=10dB)

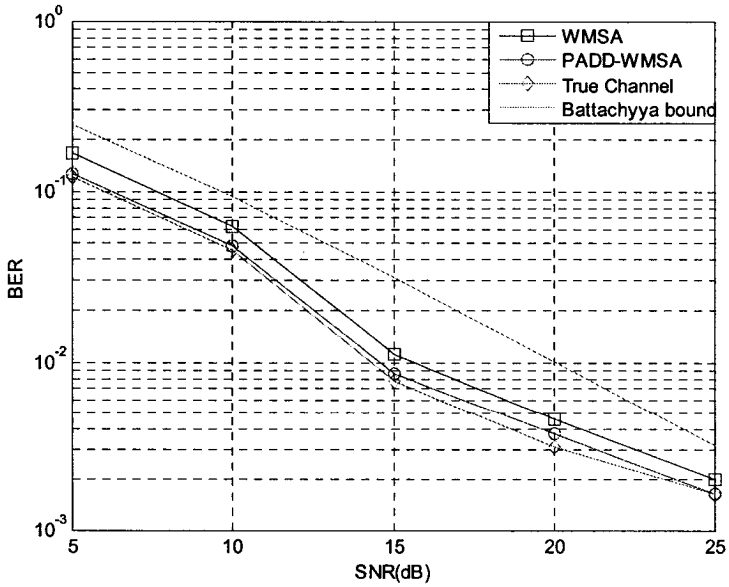

Fig. 4.10 BER performance of downlink (Velocity=120km/h)

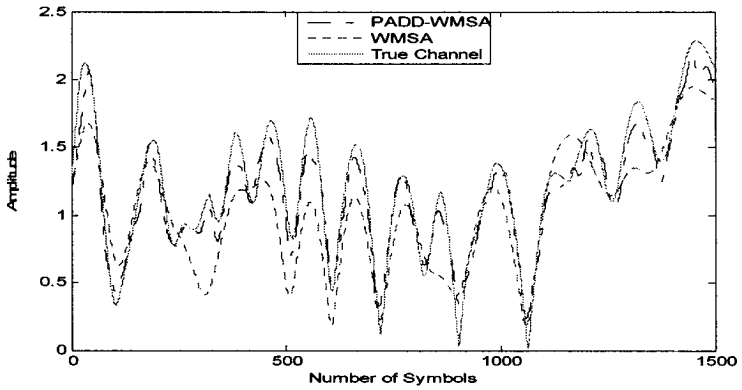

Fig. 4.11 Estimate of downlink channel amplitude (Velocity=250km/h, SNR=10dB)

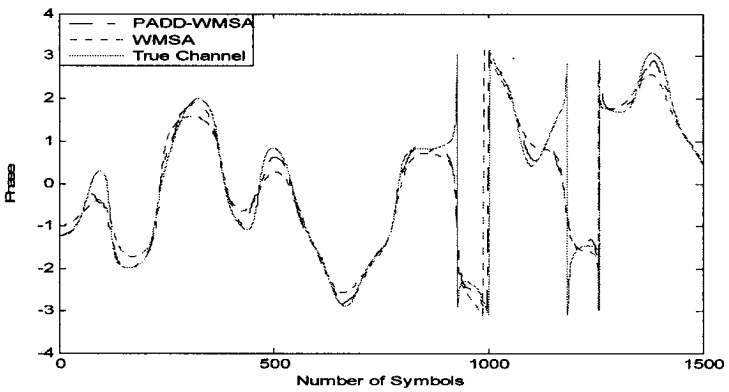

Fig. 4.12 Estimate of downlink channel phase (Velocity=250km/h, SNR=10dB)

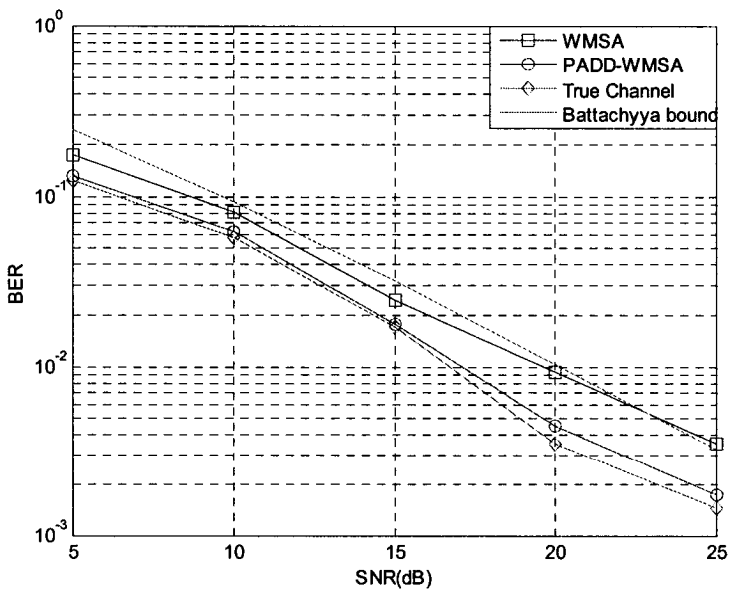

Fig. 4.13 BER performance of downlink (Velocity=250km/h)

Table 4.2 Some BER values for downlink system

SNR (dB)	BER								
	WMSA			PADD-WMSA			True channel		
	60km/h	120km/h	250km/h	60km/h	120km/h	250km/h	60km/h	120km/h	250km/h
5	0.1605	0.1672	0.1727	0.1228	0.1268	0.1315	0.1170	0.1172	0.1247
10	0.0626	0.0746	0.0816	0.0475	0.0566	0.0622	0.0452	0.0532	0.0577
15	0.0096	0.0112	0.0247	0.0076	0.0085	0.0179	0.0068	0.0077	0.0170
20	0.0048	0.0052	0.0094	0.0036	0.0039	0.0045	0.0035	0.0038	0.0038
25	0.0018	0.0021	0.0035	0.0013	0.0016	0.0018	0.0012	0.0015	0.0015

4.3.2 Simulation for WCDMA Uplink

Unlike the downlink transmission in which the TDM pilot symbols are used for channel estimation, the uplink of WCDMA systems contains continuous CDM pilot symbols to which both the WMSA and the proposed methods are also applicable. Note that the BPSK modulation scheme is specified for uplink in the WCDMA standard and the pilot and data channels of the uplink are quadraturally multiplexed. Also, the pilot channel has a fixed spreading factor of 256. Compared to the downlink where the QPSK modulation scheme is used and the pilot and data symbols are time-multiplexed, the processing gain of uplink data channels is one-half of that of the downlink data channels.

Table 4.3 lists the parameters and assumptions that are used for the modeling and simulation of the uplink system. All of these parameters are specified in the WCDMA standard [11], [35]. Similar to the downlink case, the channel estimation is conducted using the proposed scheme as well as the WMSA method for comparison. The system BER will also be computed based on the two estimation methods and the true channel

behaviour.

Table 4.3 Parameters and assumptions for uplink simulation

No.	Description	Parameters
1	Spreading code	OVSF
2	Pilot channel spreading factor	256
3	Data channel spreading factor	64
4	Data modulation	BPSK
5	Chip rate	3.84 Mchips/s
6	No. of Multi-paths	3
7	No. of Multi-paths fingers	3
8	Synchronization	Perfect
9	Path-delay	Known
10	Slot format	0B
11	Channel model	Rayleigh+Gaussian
12	Mobile velocity	60km/h,120km/h,250km/h
13	Number of users	1
14	Carrier frequency	2.14 GHz
15	WMSA Weights	$\alpha_0 = 1.0, \alpha_1 = 0.6$

The amplitude and the phase estimation results for one path are shown in Figs. 4.14 and 4.15, respectively, in conjunction with the true channel plots, for the mobile velocity of 60 km/h and the SNR of 10dB. The BER plots for the uplink system with respect to the true and the estimated channel characteristics are depicted in Fig. 4.16. These results indicate that the proposed method is slightly superior to the WMSA method although both can work well for a low mobile velocity.

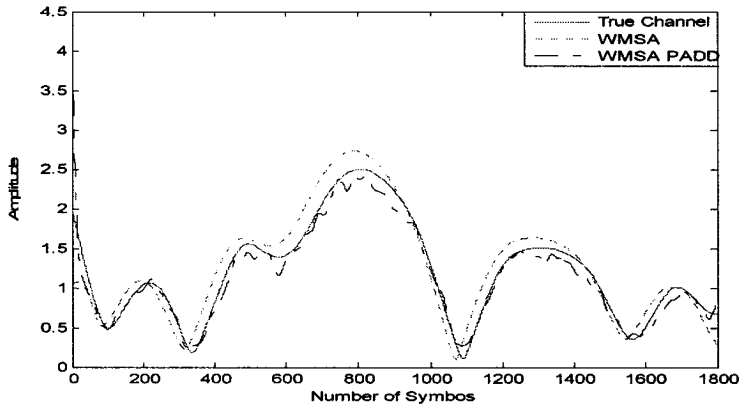

Fig. 4.14 Estimate of uplink channel amplitude (Velocity=60km/h, SNR=10dB)

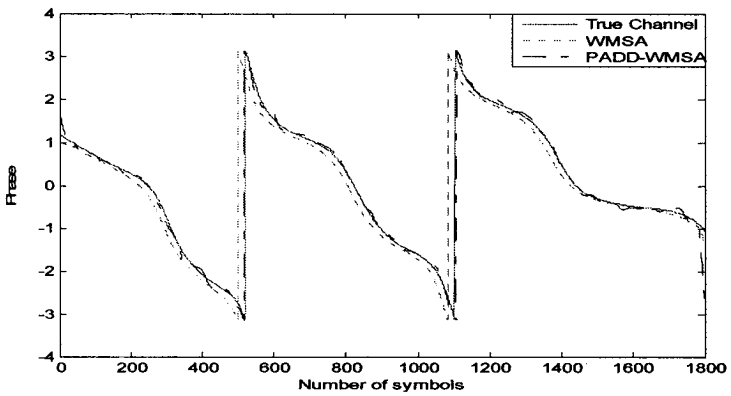

Fig. 4.15 Estimate of uplink channel phase (Velocity=60km/h, SNR=10dB)

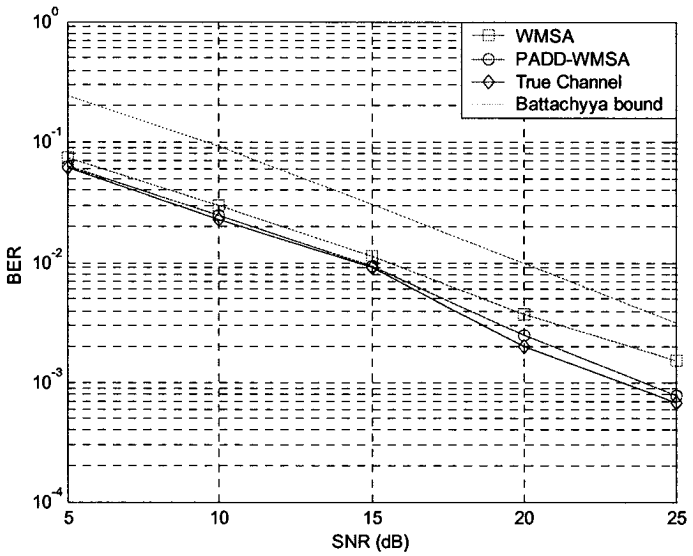

Fig. 4.16 System BER performance of uplink (Velocity=60km/h)

The simulation results with respect to the mobile velocities of 120km/h and 250km/h are shown in Figs. 4.17~4.19 and Figs. 4.20~4.22, respectively. Clearly, the proposed method is more advantageous in comparison to the WMSA method when the mobile velocity is increased, especially in the estimation of the channel amplitude. The superiority of the proposed method is obvious in terms of the BER plots shown in Figs. 4.19 and 4.22. For example, in the case of the mobile velocity of 250km/h, the WMSA method fails to provide a satisfactory estimation performance since the BER values are beyond the Battachyya bound when the SNR is above 20 dB.

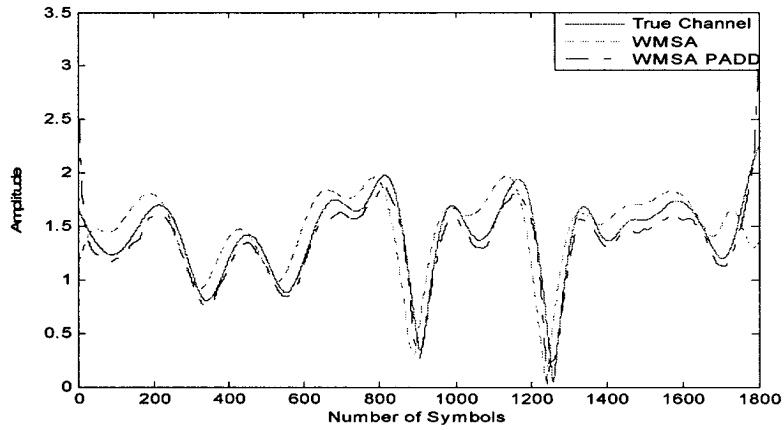

Fig. 4.17 Estimate of uplink channel amplitude (Velocity=120km/h, SNR=10dB)

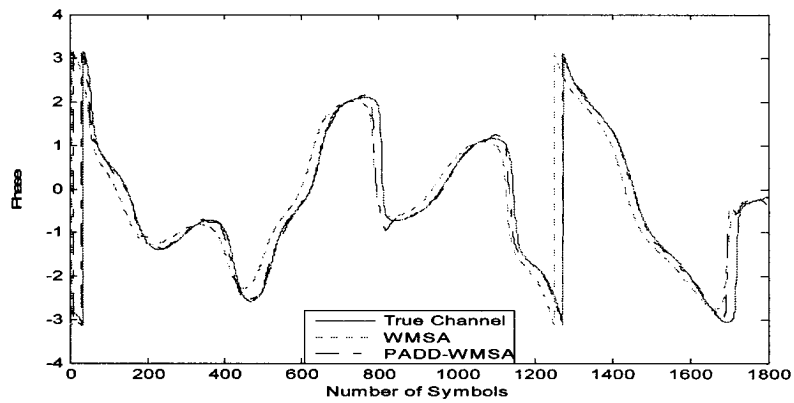

Fig. 4.18 Estimate of uplink channel phase (Velocity=120km/h, SNR=10dB)

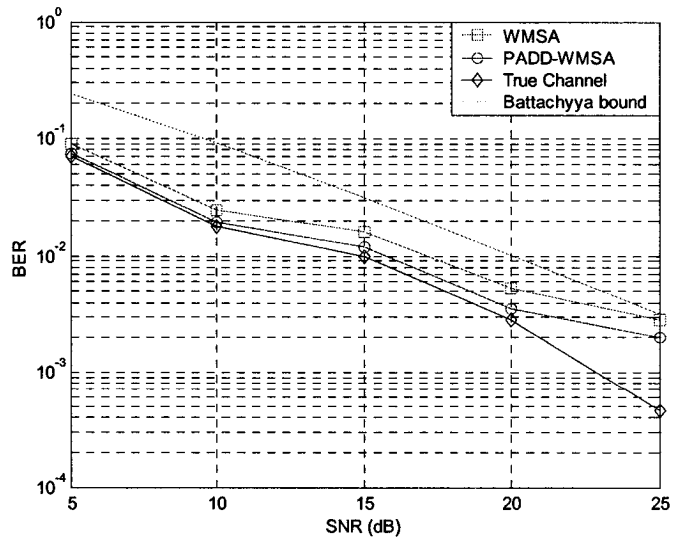

Fig. 4.19 System BER performance of uplink (Velocity=120km/h)

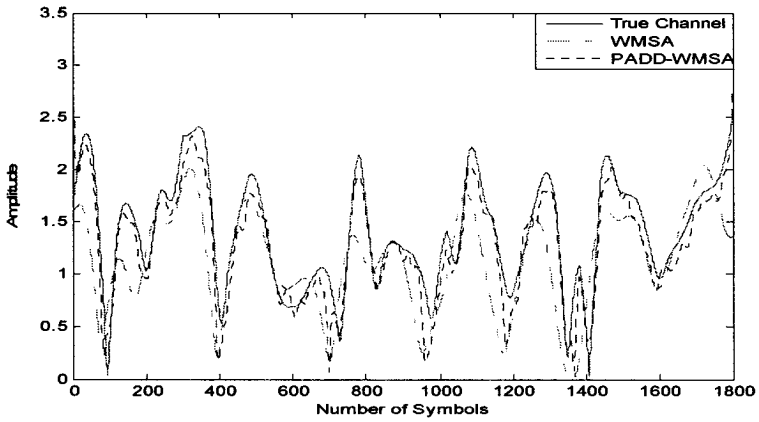

Fig. 4.20 Estimate of uplink channel amplitude (Velocity=250km/h, SNR=10dB)

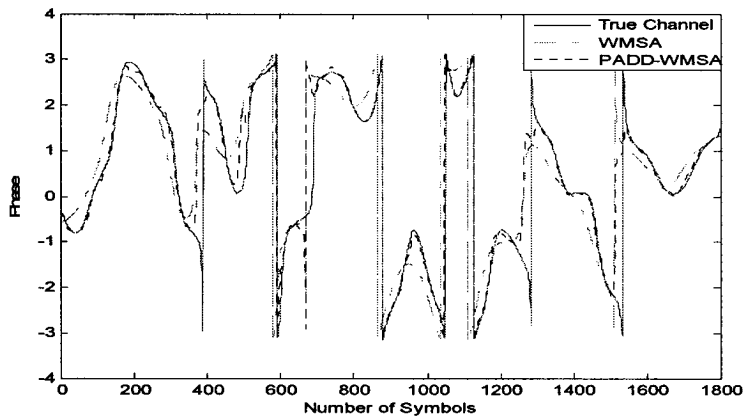

Fig. 4.21 Estimate of uplink channel phase (Velocity=250km/h, SNR=10dB)

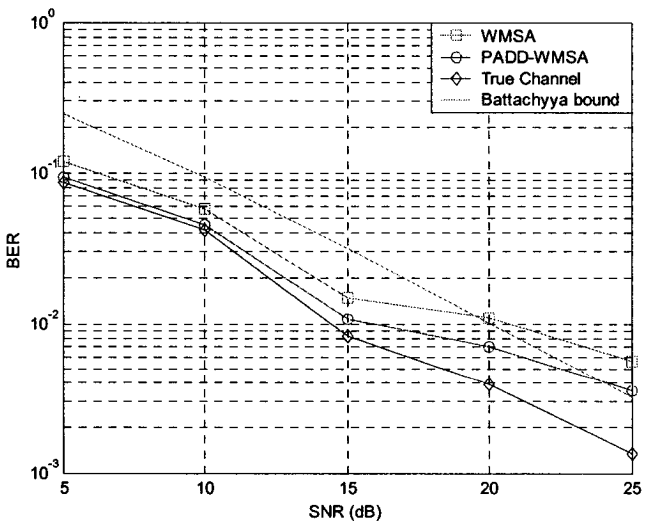

Fig. 4.22 System BER performance of uplink (Velocity=250km/h)

Table 4.4 lists some BER values for the uplink system. Comparing with Table 4.3 for BER values of the downlink system, it appears that the uplink has a better BER performance. This is because we have used different processing gains for the uplink and downlink pilot channels. The pilot channel spreading factor in the uplink is fixed at 256, while the spreading factor of the TDM pilot symbols in the downlink varies with the data rate where the spreading factor is set to 128 as a result of assuming the 60kbps data rate.

Table 4.4 Some BER values for uplink system

SNR (dB)	BER								
	WMSA			PADD-WMSA			True channel		
	60km/h	120km/h	250km/h	60km/h	120km/h	250km/h	60km/h	120km/h	250km/h
5	0.0747	0.0886	0.1274	0.0633	0.0734	0.0770	0.0740	0.0843	0.0864
10	0.0249	0.0297	0.0576	0.0193	0.0248	0.0372	0.0212	0.0271	0.0412
15	0.0113	0.0148	0.0158	0.0010	0.0089	0.0118	0.0082	0.0112	0.0118
20	0.0037	0.0053	0.0110	0.0025	0.0035	0.0058	0.0024	0.0034	0.0039
25	0.0016	0.0029	0.0056	0.0008	0.0020	0.0029	0.0006	0.0008	0.0013

4.4 Conclusion

In this chapter, a two-stage channel estimation approach referred to as the PADD-WMSA method, which combines the advantages of the decision-directed and the pilot-assisted techniques, has been proposed. In the proposed scheme, the WMSA method existing in literature has been improved by exploiting data decision symbols and an FIR smoothing filter. It has been shown through computer simulations that the proposed PADD-WMSA algorithm yields a more accurate channel estimation result and better BER performance for both downlink and uplink WCDMA systems relative to the WMSA method,

especially in fast fading environments.

It should be mentioned that as data symbols have been used to assist the channel estimation, some extra operations relating to the storage and the processing of the received data or their delayed version are needed, leading to an increase in the computational complexity. However, most of the computations incurred by the decision-directed strategy have been for the implementation of the smoothing FIR filter in the second stage and its consumption of computing resource is insignificant compared to the pilot-aided weighted averaging operations as required by the WMSA method. Therefore, the computational complexity of the proposed scheme is only slightly higher than that of the WMSA technique.

Chapter 5

Variable Step-Size Adaptive Channel Estimation

5.1 Introduction

In the last chapter, we have proposed a two-stage estimation scheme referred as PADD-WMSA for WCDMA fast fading channels. The proposed PADD-WMSA method is able to improve the system performance to a certain degree in a fast fading environment. However, it is not optimal in the sense that the coefficients of the channel estimation filter are not updated to adapt to the time-varying channel characteristics.

The best choice for the channel estimation filter for WCDMA systems is an adaptive filter due to the time-varying nature of fading channels. Generally speaking, the computational complexity of adaptive filters is higher than that of fixed-coefficient filters. Nevertheless, an adaptive filter is able to yield an optimal solution given a particular fading channel. Moreover, the state-of-the-art VLSI technology makes it possible to implement an adaptive filter in a very cost-effective fashion. Therefore, an adaptive filter using an iterative procedure for seeking the optimal coefficients is preferred provided that the implementation cost is not a major concern.

Transversal adaptive filter is one of the most commonly used adaptive filters. It uses the FIR (finite-duration impulse response) filter structure, and therefore, enjoys its stability and simple structure. A transversal adaptive filter has another advantage that its length is closely related to the convergence speed and the steady-state error of the adaptive

algorithm used, and therefore, it is relatively easy to determine the filter length according to the convergence and error requirements. This also provides a compromise between the computational complexity and the error performance, since a short filter length implies a fast convergence while it results in a large steady state error.

In recent years, a number of adaptive filtering methods have been proposed for WCDMA channel estimation. For instance, a pilot assisted and decision directed adaptive smoothing scheme for the channel characteristic has been studied in [28]. The performance study of diversity combining scheme using the minimum mean-square error (MMSE) prediction has been undertaken in [29]. Transversal filters have been used in these channel estimation methods. In general, a large filter length is necessary in order to estimate an arbitrary fading channel as accurately as possible. But a large-tap transversal filter suffers from a slow convergence. In this chapter, we propose a variable step-size adaptive scheme to improve the convergence speed while maintaining an accurate channel estimation for WCDMA systems.

5.2 Proposed Variable Step-Size Adaptive Channel Estimation Scheme

Fig. 5.1 depicts a (2N+1)-tap adaptive transversal smoothing filter proposed for WCDMA channel estimation [23, 28]. This transversal filter has been represented as a noncausal structure for notational convenience. It is, however, implemented as a causal FIR filter in practice. As shown in the figure, $\tilde{h}_n$ is the input of the adaptive filter, which represents the coarse estimate of the channel characteristic obtained from the received pilot symbols,

D the unit time delay, $w_{-N}^*,\cdots,w_{-2}^*,w_{-1}^*,w_0^*,w_1^*\cdots,w_N^*$ the complex conjugate of the $2N+1$ filter coefficients, h_n the desired channel impulse response, e_n the estimation error between the desired channel response and the filtered estimate $\hat{h}_n$. Note that in a multipath fading environment, each fading path requires an individual smoothing filter, namely, the structure in Fig. 5.1 is considered for one path only.

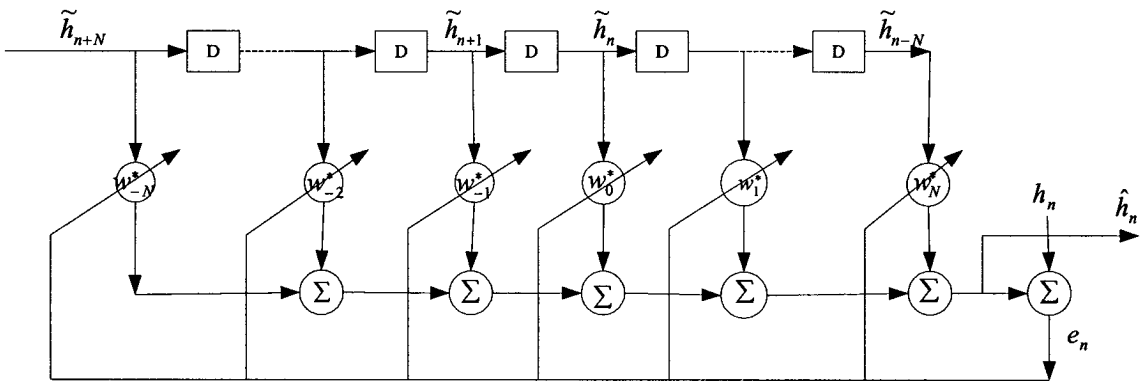

Fig. 5.1 Adaptive transversal smoothing filter for channel estimation

From Fig.5.1, the filtered channel estimate can be written as

$$\hat{h}_n = \sum_{k=-N}^{k=N} w_k^* \tilde{h}_{n-k} = \mathbf{w}_n^H \tilde{\mathbf{h}}_n \tag{5.1}$$

where $(\cdot)^*$ denotes the complex conjugate, $(\cdot)^H$ the conjugate transpose, and $\mathbf{w}_n$ and $\tilde{\mathbf{h}}_n$ represent, respectively, the filter coefficient vector and the input coarse estimate vector of the adaptive filter at time n as given by

$$\mathbf{w}_n = \begin{pmatrix} w_{-N} & \cdots & w_{-1} & w_0 & w_1 & \cdots & w_N \end{pmatrix}^T, \tag{5.2}$$

$$\tilde{\mathbf{h}}_n = \begin{pmatrix} \tilde{h}_{n+N} & \cdots & \tilde{h}_{n+1} & \tilde{h}_n & \tilde{h}_{n-1} & \cdots & \tilde{h}_{n-N} \end{pmatrix}^T. \tag{5.3}$$

The optimal closed-form solution for the coefficient vector in the MMSE sense, namely, the Wiener solution, can be written as [18]

$$\mathbf{w}_{opt} = \left[E(\tilde{\mathbf{h}}_n \tilde{\mathbf{h}}_n^H)\right]^{-1} E\left[\tilde{\mathbf{h}}_n \mathbf{h}_n^H\right] \tag{5.4}$$

Computation of the Wiener solution (5.4) is not straightforward due to some difficulties in obtaining a good estimate of the correlation matrix as well as the desired signal or the ideal channel response. The principle of adaptive prediction can be used to attain the coefficients of the adaptive smoothing filter [28], where one attempts to predict the actual channel response from the input coarse samples $\tilde{h}_n$. Adaptive linear prediction is known to be very useful in spectral analysis for many years. In what follows, we will investigate the application of the linear prediction method in the estimation of multipath fading channels.

According to the prediction theory, the estimate of the fading distortion h_n can be represented as [28]

$$\hat{h}_n = \sum_{k=-N, n\neq 0}^{k=N} w_k^* \tilde{h}_{n-k} \,. \tag{5.5}$$

The estimation error can be written as

$$e_n = h_n - \hat{h}_n \,. \tag{5.6}$$

Then, the update formula for the coefficient vector of the adaptive filter can be given by

$$\begin{aligned} \mathbf{w}_{n+1} &= \mathbf{w}_n + \mu e_n^* \tilde{\mathbf{h}}_n \\ &= \mathbf{w}_n + \mu (h_n - \hat{h}_n)^* \tilde{\mathbf{h}}_n \end{aligned} \tag{5.7}$$

where μ is the step-size. The choice of filter length $2N+1$ is a key to the implementation of the channel estimator in view of the estimation accuracy. Ideally, the value of N should be infinity in order to cover all possible time-varying characteristics of the channel, which is obviously unrealistic. Generally speaking, a practical channel response

should have an energy that is concentrated in a relatively short period of time near the beginning of the response. Thus, the "tail' of the channel response, which is considered to convey much less energy, can be neglected. However, this situation may not be true for WCDMA communication systems, where the multi-path channels have a widely spread signal energy. Moreover, multi-path channels have the nature of time-variation and may appear as slow fading or fast fading channel depending on the velocity of the mobile terminal. Accordingly, the channel estimation filter should work well for a wide range of channel characteristics. Therefore, a relatively large value for N is necessary for WCDMA channel estimation. But, a large filter length would slow down the convergence of the adaptive algorithm. In order to speed up the convergence of the adaptive filter with large taps, we propose a variable step-size adaptive channel estimation algorithm. In what follows, we will firstly analyze the relationship between convergence speed and the step-size, and then present a simplified variable step-size adaptive channel estimation method.

5.2.1 Relationship between Convergence Speed and Step-Size

In the algorithmic analysis, we omit the additive noise since it is independent of the channel response as well as the adaptive filter coefficients and thus it does not have large impact on the convergence speed. However, the additive noise makes a main contribution to the steady state error, and it should not be neglected in the simulation of the algorithm.

Assume that the channel impulse response h_n is statistically independent of the filter weight $\mathbf{w}_n$, and $\mathbf{g}_n$ represents the impulse response of the desired ideal infinite-length filter with which the true channel response can be obtained from $\tilde{h}_n$ [12], [43], i.e.,

$$h_n = \sum_{k=-\infty}^{k=+\infty} g_k^* \tilde{h}_{n-k} . \tag{5.8}$$

On the other hand, the output of the (2N+1)-tap adaptive filter, i.e., the estimate of the true channel response is given by (5.5). The estimation error can then be written as

$$e_n = h_n - \hat{h}_n = (\mathbf{g} - \mathbf{w})^H \tilde{\mathbf{h}}_n + \sum_{k=-\infty}^{-(N+1)} g_k^* \tilde{h}_{n-k} + \sum_{k=N+1}^{+\infty} g_k^* \tilde{h}_{n-k} , \tag{5.9}$$

where

$$\mathbf{g} = [g_{-N}, \ldots, g_0, \ldots, g_N]^T ,$$

$$\mathbf{w} = [w_{-N}, \ldots, w_0, \ldots, w_N]^T ,$$

$$\tilde{\mathbf{h}}_n = [\tilde{h}_{n+N}, \ldots, \tilde{h}_n, \ldots, \tilde{h}_{n-N}]^T .$$

Denote the last two terms in (5.9) as ρ_n, which represents the partial channel estimation error. Note that it has zero mean as long as the estimation is unbiased. This error depends on the length of the adaptive filter and is irreducible since it cannot be estimated once the length of the adaptive filter is fixed. Clearly, one can decrease the partial error by increasing the estimation filter length. Let us assume the variance of ρ_n to be σ_ρ^2, and the variance of the input channel estimate to be σ_h^2. Assuming that $\mathbf{w}_n$ and $\tilde{\mathbf{h}}_n$ are statistically independent [12], [43], the mean squared channel estimation error can be written as

$$\varepsilon_n = E[e_n \cdot e_n^*] = E[(\mathbf{g} - \mathbf{w}_n)^H \tilde{\mathbf{h}}_n \tilde{\mathbf{h}}_n^H (\mathbf{g} - \mathbf{w}_n)] + \sigma_\rho^2 . \tag{5.10}$$

In most practical wireless channels, the coefficients of the channel response are highly

uncorrelated with each other [1]. Furthermore, in commonly used channel models, such as Clarke's model, the channel response is assumed to be independent at different time instants. Accordingly, it is reasonable to assume that $\tilde{\mathbf{h}}_n$ is a white process, leading to

$$\begin{aligned}\varepsilon_n &= E[(\mathbf{g}-\mathbf{w}_n)^H E(\tilde{\mathbf{h}}_n\tilde{\mathbf{h}}_n^H)(\mathbf{g}-\mathbf{w}_n)] + \sigma_\rho^2 \\ &= \sigma_h^2 E[(\mathbf{g}-\mathbf{w}_n)^H(\mathbf{g}-\mathbf{w}_n)] + \sigma_\rho^2\end{aligned} \tag{5.11}$$

Given the length of the adaptive filter, only the first term in the right-hand side of (5.11) can be decreased and it can be denoted as ε_n^r, i.e.,

$$\varepsilon_n^r = \sigma_h^2 E[(\mathbf{g}-\mathbf{w}_n)^H(\mathbf{g}-\mathbf{w}_n)]. \tag{5.12}$$

The filter coefficient vector can be updated using (5.7) as given below,

$$\mathbf{w}_{n+1} = \mathbf{w}_n + \mu e_n^* \tilde{\mathbf{h}}_n \tag{5.13}$$

Applying (5.13) to (5.12), one can compute the reducible part of the mean square error at time $(n+1)$ as given by

$$\begin{aligned}\varepsilon_{n+1}^r &= \sigma_h^2 E[(\mathbf{g}-\mathbf{w}_{n+1})^H(\mathbf{g}-\mathbf{w}_{n+1})] \\ &= \sigma_h^2 E[((\mathbf{g}-\mathbf{w}_n)-\mu e_n^*\tilde{\mathbf{h}}_n)^H((\mathbf{g}-\mathbf{w}_n)-\mu e_n^*\tilde{\mathbf{h}}_n)] \\ &= \sigma_h^2 E[(\mathbf{g}-\mathbf{w}_n)^H(\mathbf{g}-\mathbf{w}_n)] \\ &\quad -\mu\sigma_h^2 E[(\mathbf{g}-\mathbf{w}_n)^H e_n^*\tilde{\mathbf{h}}_n] - \mu\sigma_h^2 E[e_n\tilde{\mathbf{h}}_n^H(\mathbf{g}-\mathbf{w}_n)] + \mu^2\sigma_h^2 E[e_n\cdot e_n^*\tilde{\mathbf{h}}_n^H\tilde{\mathbf{h}}_n]\end{aligned} \tag{5.14}$$

Using (5.9) into the second and the third terms in the right side of (5.14), we can get

$$\begin{aligned}\mu\sigma_h^2 E[(\mathbf{g}-\mathbf{w}_n)^H e_n^*\tilde{\mathbf{h}}_n] &= \mu\sigma_h^2 E[(\mathbf{g}-\mathbf{w}_n)^H\tilde{\mathbf{h}}_n e_n^*] \\ &= \mu\sigma_h^2 E[(\mathbf{g}-\mathbf{w}_n)^H\tilde{\mathbf{h}}_n((\mathbf{g}-\mathbf{w}_n)^H\tilde{\mathbf{h}}_n+\rho_n)^*] \\ &= \mu\sigma_h^2 E[(\mathbf{g}-\mathbf{w}_n)^H\tilde{\mathbf{h}}_n\tilde{\mathbf{h}}_n^H(\mathbf{g}-\mathbf{w}_n)+\rho_n^*(\mathbf{g}-\mathbf{w}_n)^H\tilde{\mathbf{h}}_n]\end{aligned} \tag{5.15}$$

and

$$\begin{aligned}\mu\sigma_h^2 E[e_n\tilde{\mathbf{h}}_n^H(\mathbf{g}-\mathbf{w}_n)] &= \mu\sigma_h^2 E[((\mathbf{g}-\mathbf{w}_n)^H\tilde{\mathbf{h}}_n+\rho_n)\tilde{\mathbf{h}}_n^H(\mathbf{g}-\mathbf{w}_n)] \\ &= \mu\sigma_h^2 E[(\mathbf{g}-\mathbf{w}_n)^H\tilde{\mathbf{h}}_n\tilde{\mathbf{h}}_n^H(\mathbf{g}-\mathbf{w}_n)+\rho_n\tilde{\mathbf{h}}_n{}^H(\mathbf{g}-\mathbf{w}_n)]\end{aligned} \tag{5.16}$$

Taking into account the assumption that ρ_n (with zero-mean) is independent of $\tilde{h}_n$ and the filter tap w_n, (5.15) and (5.16) can be combined as

$$\begin{aligned}
&\mu\sigma_h^2 E[(\mathbf{g}-\mathbf{w}_n)^H \tilde{\mathbf{h}}_n \tilde{\mathbf{h}}_n^H (\mathbf{g}-\mathbf{w}_n) + \rho_n^* (\mathbf{g}-\mathbf{w}_n)^H \tilde{\mathbf{h}}_n] \\
&+ \mu\sigma_h^2 E[(\mathbf{g}-\mathbf{w}_n)^H \tilde{\mathbf{h}}_n \tilde{\mathbf{h}}_n^H (\mathbf{g}-\mathbf{w}_n) + \rho_n \tilde{\mathbf{h}}_n^H (\mathbf{g}-\mathbf{w}_n)] \\
&= 2\mu\sigma_h^2 \sigma_h^2 E[(\mathbf{g}-\mathbf{w}_n)^H (\mathbf{g}-\mathbf{w}_n)] \\
&= 2\mu\sigma_h^2 \varepsilon_n^r
\end{aligned} \tag{5.17}$$

The fourth term in the right side of (5.14) becomes

$$\mu^2\sigma_h^2 E[e_n \cdot e_n^* \tilde{\mathbf{h}}_n^H \tilde{\mathbf{h}}_n] = \mu^2\sigma_h^2\sigma_h^2 E[e_n \cdot e_n^*] = \mu^2\sigma_h^4(\varepsilon_n^r + \sigma_\rho^2) \tag{5.18}$$

Substituting (5.17) and (5.18) into (5.14) yields

$$\begin{aligned}
\varepsilon_{n+1}^r &= \varepsilon_n^r - 2\mu\sigma_h^2\varepsilon_n^r + \mu^2\sigma_h^4\varepsilon_n^r + \mu^2\sigma_h^4\sigma_\rho^2 \\
&= (1 - 2\mu\sigma_h^2 + \mu^2\sigma_h^4)\varepsilon_n^r + \mu^2\sigma_h^4\sigma_\rho^2 \\
&= (1-\mu\sigma_h^2)^2 \varepsilon_n^r + \mu^2\sigma_h^4\sigma_\rho^2
\end{aligned} \tag{5.19}$$

which can be written in the update form as

$$\varepsilon_{n+1}^r = a\varepsilon_n^r + b$$

with

$$a = (1-\mu\sigma_h^2)^2$$

$$b = \mu^2\sigma_h^4\sigma_\rho^2$$

Thus, using the initial error ε_0^r, we have

$$\varepsilon_{n+1}^r = a^{n+1}\varepsilon_0^r + b\left(\sum_{i=0}^{n} a^i\right) = a^{n+1}\left[\varepsilon_0^r - \frac{b}{1-a}\right] + \frac{b}{1-a} \tag{5.20}$$

Substituting the values of a and b into (5.20), we obtain

$$\begin{aligned}\varepsilon_{n+1}^{r} &= (1-\mu\sigma_h^2)^{2(n+1)}\left[\varepsilon_0^r - \frac{\mu^2\sigma_h^4\sigma_\rho^2}{1-(1-\mu\sigma_h^2)^2}\right] + \frac{\mu^2\sigma_h^4\sigma_\rho^2}{1-(1-\mu\sigma_h^2)^2} \\ &= (1-\mu\sigma_h^2)^{2(n+1)}\left[\varepsilon_0^r - \frac{\mu\sigma_h^2\sigma_\rho^2}{2-\mu\sigma_h^2}\right] + \frac{\mu\sigma_h^2\sigma_\rho^2}{2-\mu\sigma_h^2}\end{aligned} \tag{5.21}$$

It is clearly seen from (5.21) that the convergence speed of the adaptive channel estimation filter depends on the step-size μ and the variance σ_h^2. It can also be observed that in order to optimize the convergence speed, the step-size should be a variable and adjustable in each iteration.

5.2.2 Simplified Variable Step-Size Channel Estimation Algorithm

The optimal convergence speed with respect to the step-size μ could be obtained by minimizing (5.21) in each iteration. However, this may not be practical or even impossible, since it is a time-consuming process to find the optimal step-size μ such that (5.21) is minimized in each iteration. On the other hand, if the step-size is set as a fixed value, an overall computational complexity can be obtained. However, the convergence may not be fast. Therefore, choosing a proper step-size μ is a key issue in adaptive channel estimation algorithm. In what follows, we will propose a simplified variable step-size scheme to comprise the convergence speed and the algorithmic complexity.

It is well known that in order to ensure the convergence of a $(2N+1)$-tap adaptive filter, there exists an upper bound for the choice of the step-size μ [33], that is,

$$0 < \mu < \frac{1}{(2N+1)\sigma_h^2} \tag{5.22}$$

We use the upper bound of the step-size μ first in the updating process, that is

$$\mu = \frac{1}{(2N+1)\sigma_h^2} \tag{5.23}$$

Using (5.23) into (5.21), after some simple manipulations, we obtain

$$\varepsilon_{n+1}^r = \left(1 - \frac{1}{(2N+1)}\right)^{2(n+1)} \left(\varepsilon_0^r - \frac{\sigma_\rho^2}{4N+1}\right) + \frac{\sigma_\rho^2}{4N+1} \tag{5.24}$$

For a practical wireless channel, one can take a reasonable value of N such that $4N+1 >> \sigma_\rho^2$. Then (5.24) can be simplified as

$$\varepsilon_{n+1}^r \cong \left(1 - \frac{1}{(2N+1)}\right)^{2(n+1)} \varepsilon_0^r \tag{5.25}$$

With the step-size given by (5.23), the above mean square error tends to be zero as the number of iterations gets infinite, and the error ε_n given by (5.10) is reduced to the irreducible part σ_ρ^2. It is also clear from (5.25) that the dependence of the error ε_{n+1}^r on the filter length is straightforward. Choosing a smaller filter length would decrease the factor $(1-1/(2N+1))$ and therefore, would speed up the convergence process. However, a small filter length yields a large irreducible error σ_ρ^2.

Table 5.1 lists the convergence speed for different choices of the filter length and step-size in terms of the number of iterations for which the MSE given by (5.25) has reached 0.01. It is seen that with the increase of the filter length the step-size decreases while the convergence speed slows down. From the convergence speed point of view, we should use a small-tap estimation filter. On the other hand, as seen from (5.9), the irreducible error will decrease when the filter length increases, implying that we should

use a large-tap estimation filter in order to reduce the mean square error. As a consequence, the step-size is the main factor affecting the convergence speed and the irreducible error.

Table 5.1 Convergence speed for different filter lengths and step-sizes

Filter length	Step-size	Iteration number
13	0.0769	28
23	0.0434	51
33	0.0303	73
43	0.0232	96
53	0.0188	119

From the above observation, we propose to use a small-length transversal filter at the beginning of the iterative LMS algorithm in order to achieve a fast initial convergence. Then, the filter length and/or the step-size of the LMS algorithm will be adjusted as the iteration goes on. The proposed adaptive process can be divided into two stages as shown in Fig. 5.2 and Fig. 5.3.

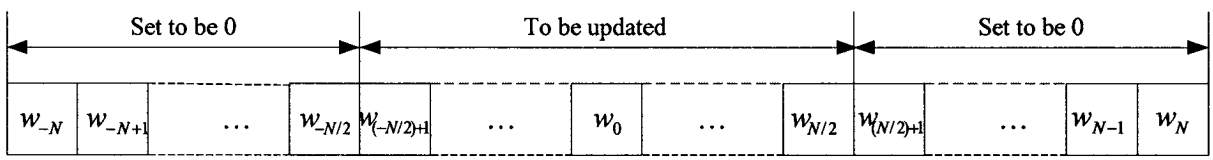

Fig. 5.2 Update scheme for the first stage of the proposed algorithm

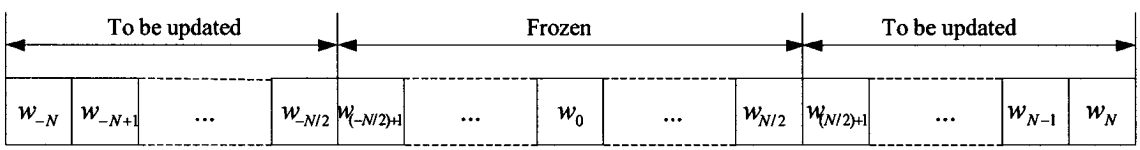

Fig. 5.3 Update scheme for the second stage of the proposed algorithm

In the first stage, only $(2N_1+1)$ out of $(2N+1)$ coefficients are to be updated. In our simulation, we choose $N_1 = N/2$. The rest of the coefficients are set to zero. After a number of iterations when the mean square error is already reduced to certain level, we switch to the second-stage of the algorithm to update the other half coefficients. In different stages, we use different step-sizes to achieve a good compromise between the convergence speed and the steady state error.

It should be mentioned that the overall convergence speed mainly depends on the step-size utilized in the first stage, which can be determined from the length $(2N_1+1)$ according to (5.24). The step-size can be chosen to be larger than that for (2N+1)-tap filter because of $N_1 < N$. Consequently, the convergence speed in the first stage is much faster than the original constant step-size (2N+1)-tap filter. It is also interesting to note that the irreducible error is mainly determined by the final step-size μ_{final} used in the second stage. Since the major filter coefficients have been adjusted to its target values in the first stage, the irreducible error can be smaller than the original large-tap constant step-size filter. Another remark is worthy to be made. The solution of the proposed variable step-size adaptive channel estimation is suboptimal in view of the full-length filter. After the iterations in the first stage, the filter coefficients will be frozen in the second-stage iterations. Thus, the variable step-size adaptive filter is not globally optimal for all coefficients and the consequence is that the channel estimation performance may be slightly degraded. However, this suboptimality does not considerably affect the overall performance of the communication system since in wireless channels, particularly in fast

fading channels, a fast estimation of the channel characteristic, even though the estimation is suboptimal, is more important than the optimality of the estimation result.

Selection of filter taps is another issue in the proposed adaptive algorithm. One solution is to use the method proposed in [34] to adjust the filter order automatically but it is very complex in implementation. In our experimentation, we have attempted various filter lengths for different fading situations including slow fading and fast fading. We have found that a filter length between 30 and 40 is sufficient for a very precise estimation.

5.3 Simulation Results

In this section, the proposed variable step-size adaptive channel estimation scheme is simulated for the WCDMA uplink system, showing the convergence plot of the mean square error, the amplitude and phase estimates of the fading channel as well as the BER performance of the system. The proposed scheme is also compared with the conventional constant step-size adaptive algorithm in terms of the simulation results.

The simulation parameters and conditions that are used for the system modeling and simulation are similar to those used in Chapter 4, and are listed in Table 5.2. Table 5.3 and Table 5.4 show, respectively, the parameters of the constant step-size adaptive filter and those of the variable step-size filter.

Table 5.2 Parameters and assumptions for uplink simulation

No.	Description	Parameters
1	Spreading code	OVSF
2	Pilot channel spreading factor	256
3	Data channel spreading factor	64
4	Data modulation	BPSK
5	Chip rate	3.84 Mchips/s
6	No. of Multi-paths	3
7	No. of fingers	3
8	Synchronization	Perfect
9	Path-delay	Known
10	Slot format	0B
11	Channel model	Rayleigh+Gaussian
12	Mobile velocity	60km/h,120km/h,250km/h
13	Number of users	1
14	Carrier frequency	2.14 GHz

Table 5.3 Parameters of constant step-size adaptive filter

Items	Parameter
Filter length	33
Step-size	0.02

Table 5.4 Parameters of variable step-size adaptive filter

Items	Parameter
Full filter length	33
Adjusted number of coefficients in first stage	17
Adjusted number of coefficients in second stage	16
Step-size	$\mu 1 = 0.05$
	$\mu 2 = 0.01$

Fig. 5.4 shows the learning curve of the MSE resulting from the proposed variable

step-size adaptive filter as well as that from the conventional constant step-size adaptive filter. In this simulation, the mobile velocity is fixed at 60 km/h and the SNR at 10dB. The estimated amplitude and phase of the channel for one path are shown in Figs. 5.5 and 5.6, respectively, and the corresponding BER performance is given in Fig. 5.7. It is clear that the proposed variable step-size filter has a much faster convergence and a smaller steady-state MSE compared to the constant step-size filter. The amplitude and phase estimates resulting from the proposed adaptive scheme are also closer to the true channel characteristics in comparison to the constant step-size algorithm. Note that both the adaptive schemes lead to a similar BER performance for the uplink system. This is due to the fact that the BER performance would not be affected by the channel estimation precision provided that the estimate of the channel response is sufficiently accurate for correct symbol decision.

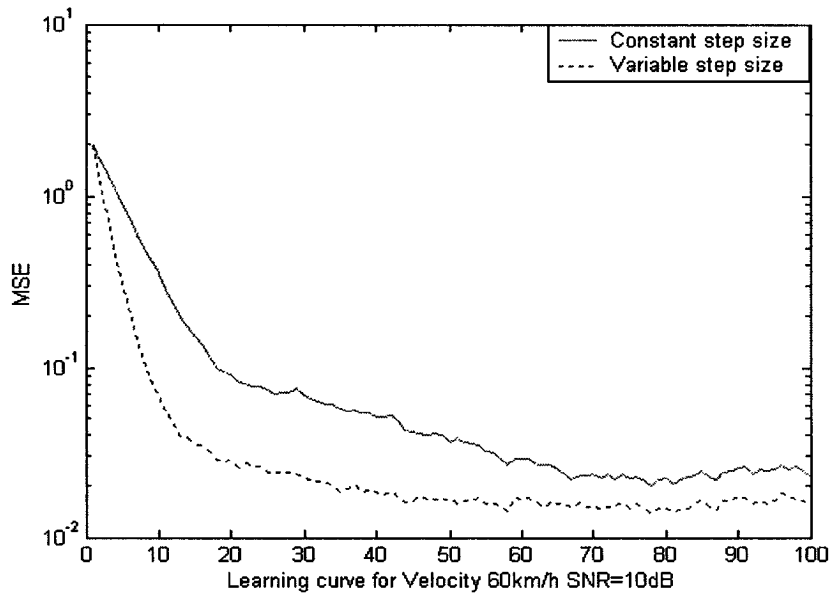

Fig. 5.4 Convergence curve of MSE (Velocity=60km/h)

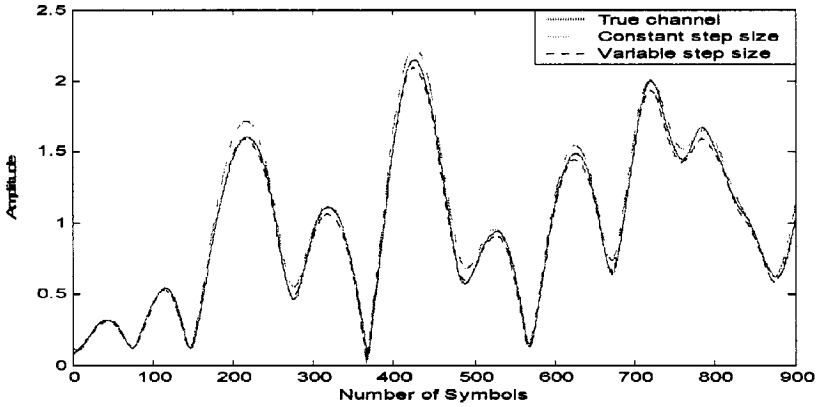

Fig. 5.5 Estimated channel amplitude using adaptive filter (Velocity=60km/h)

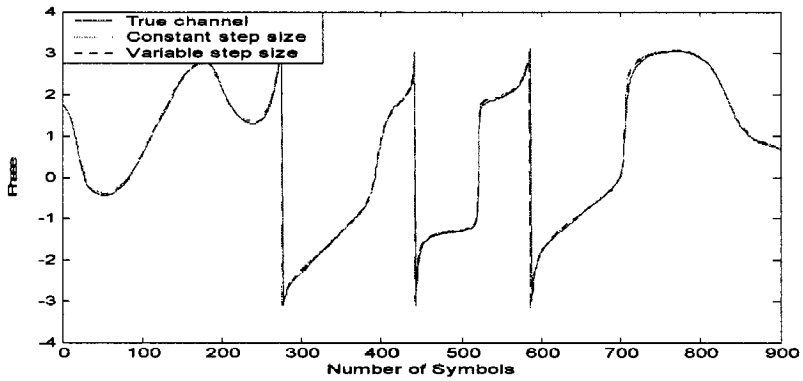

Fig. 5.6 Estimated channel phase using adaptive filter (Velocity=60km/h)

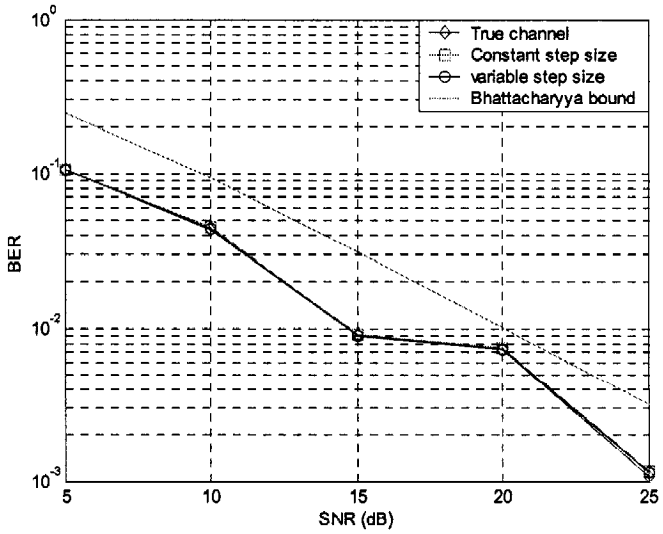

Fig. 5.7 BER plot of uplink system using adaptive filter (Velocity =60km/h)

The simulation results regarding the mobile velocity of 120km/h are shown in Figs. 5.8-5.11, where the SNR is again set to 10 dB. Similar to the case of mobile velocity being 60 km/h, the proposed variable step-size adaptive scheme is superior to the constant step-size scheme in both convergence speed and estimation performance. However, the overall convergence speed for 120km/h mobile terminal is slightly slower than that for 60 km/h terminal no matter whether the constant or the variable step-size scheme is employed.

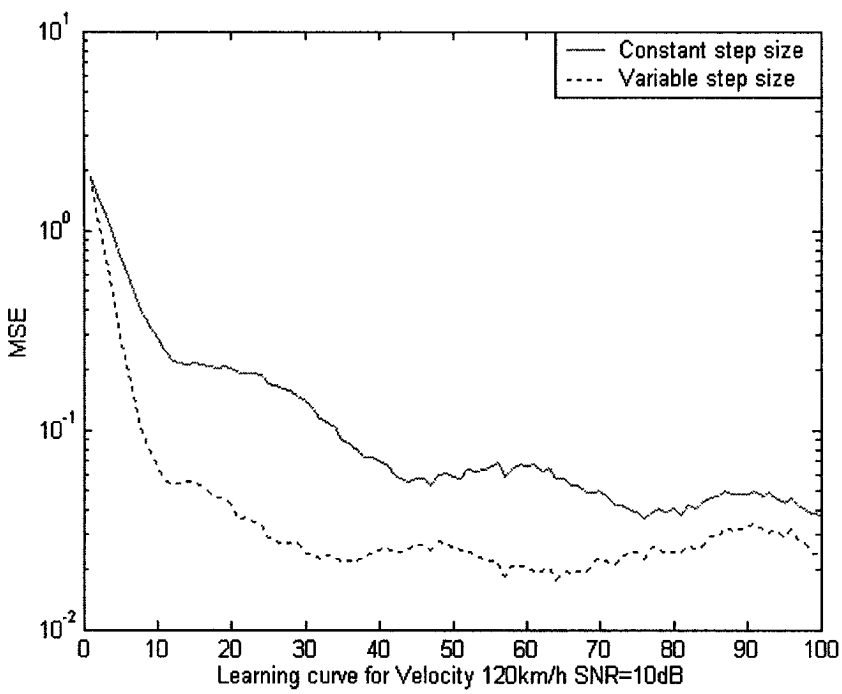

Fig. 5.8 Convergence curve of MSE (Velocity=120km/h)

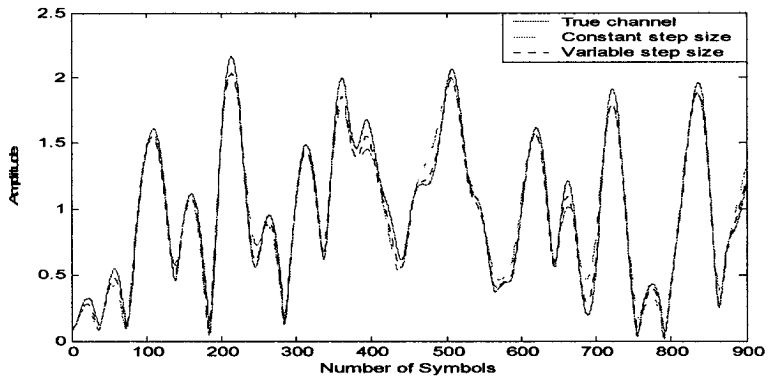

Fig. 5.9 Estimated channel amplitude using adaptive filter (Velocity =120km/h)

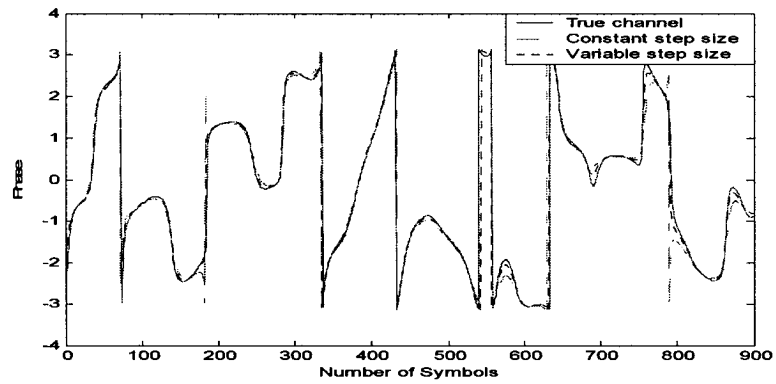

Fig. 5.10 Estimated channel phase using adaptive filter (Velocity=120km/h)

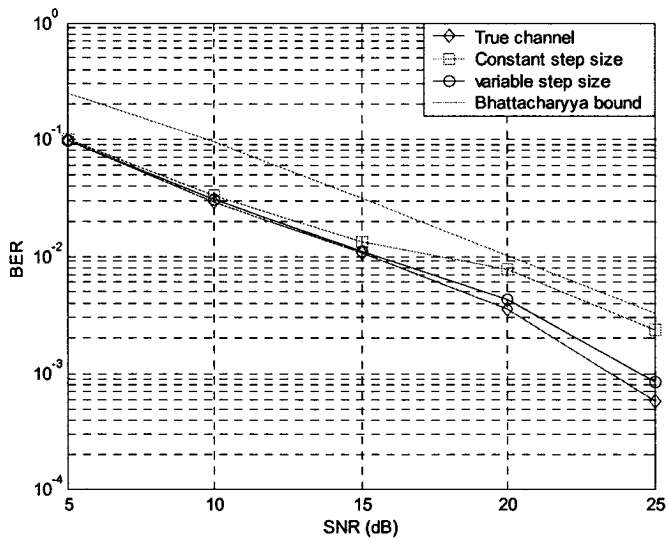

Fig. 5.11 BER plot of uplink system using adaptive filter (Velocity=120km/h)

Figs. 5.12-5.15 depict the simulation results corresponding to 250km/h mobile velocity and 10 dB SNR. It is noted that the proposed scheme has a slightly faster convergence and almost the same steady-state error in comparison to the conventional constant step-size algorithm. It is also seen from Figs. 5.13 and 5.14 that the estimation becomes less accurate for both schemes as the mobile speed increases. This is because of the different changing rate of the channel response under different mobile velocities. At a low velocity, the channel varies slowly and the channel response doesn't change significantly in a short period of time. Therefore, the adaptive filter is able to track the channel variation well, yielding an accurate estimation result. With the increase of mobile velocity, the channel variation becomes faster, making it more difficult for the adaptive filter to follow and thus leading to less accurate estimation results. A similar observation can be made to the BER performance shown in Fig. 5.15, namely, the BER gets degraded as the mobile velocity is increased.

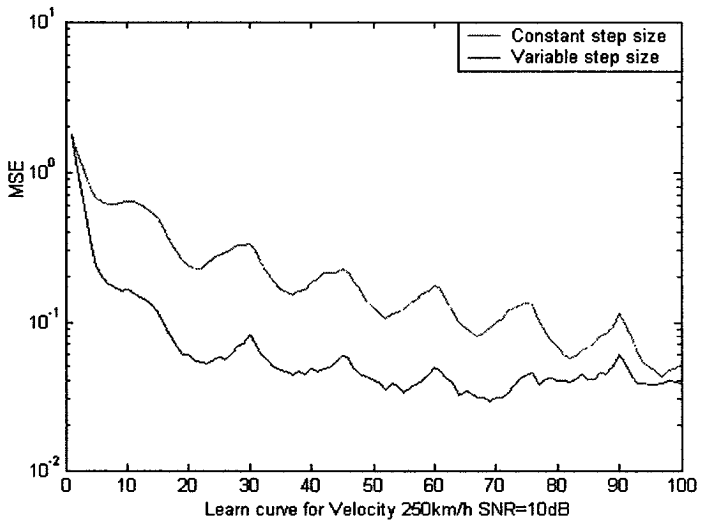

Fig. 5.12 Convergence curve of MSE (Velocity=250km/h)

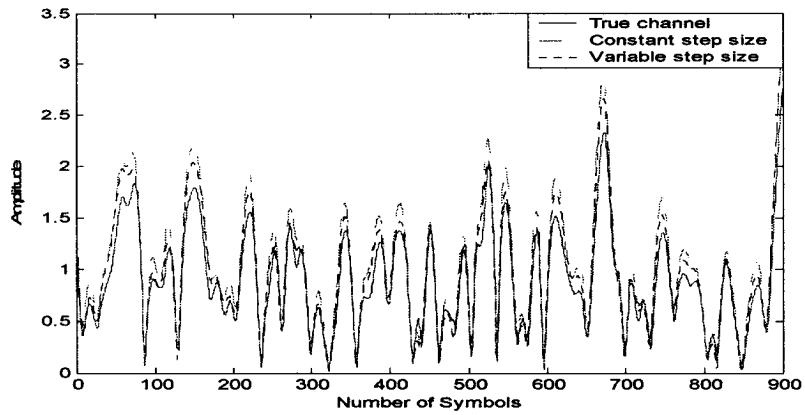

Fig. 5.13 Estimated channel amplitude using adaptive filter (Velocity=250km/h)

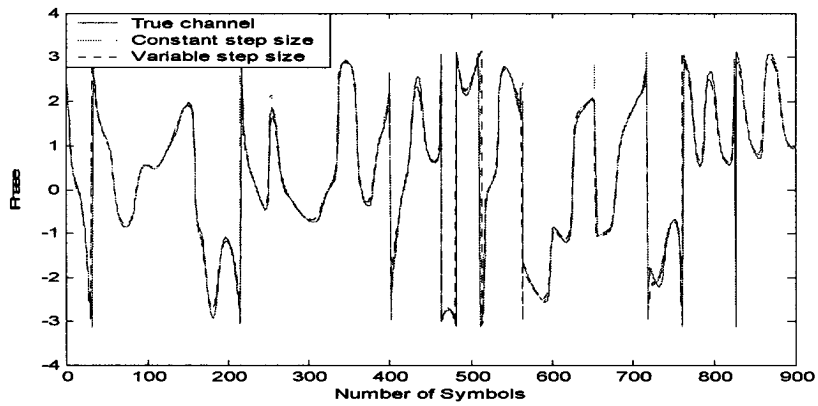

Fig. 5.14 Estimated channel phase using adaptive filter (Velocity=250km/h)

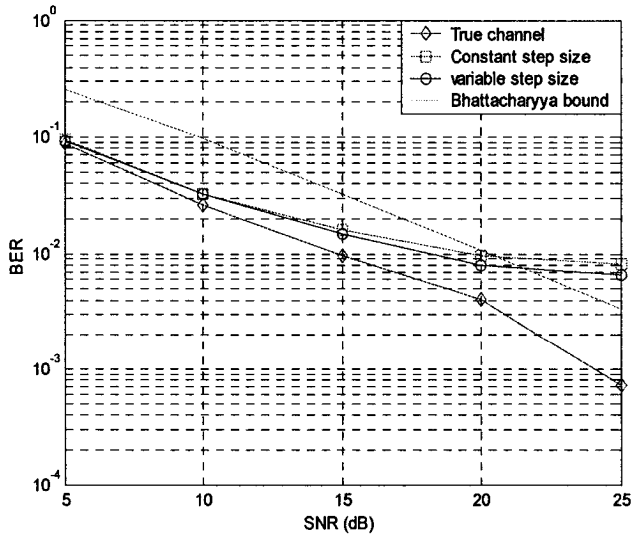

Fig. 5.15 BER plot of uplink system using adaptive filter (Velocity=250km/h)

5.4 Conclusion

In this chapter, we have proposed an efficient channel estimation method that uses a variable step-size adaptive transversal filter. The theoretical analysis of the LMS algorithm for the channel estimation problem has shown that the convergence rate of the adaptive filter mainly depends on the filter length and the step-size, and the mean squared error can be explicitly expressed in terms of the filter length. It has also been shown that the convergence can be accelerated by using a large step-size at an early stage of the adaptive filtering, and in the mean time, the steady-state error can be reduced to a satisfactory degree by employing a small step-size at a late stage of the update algorithm. The proposed method has been simulated and compared with the conventional constant step-size adaptive algorithm for WCDMA uplink channel estimation. Our simulation has shown that the proposed channel estimation method outperforms the conventional one using a constant step-size adaptive procedure.

Chapter 6

Conclusion and Future Work

6.1 Concluding Remarks

In this thesis, a few new channel estimation techniques have been proposed for WCDMA systems. A theoretical analysis and detailed simulation study have been carried out to show the estimation performance of the proposed techniques as well as the BER performance of the WCDMA systems with the proposed channel estimation for different mobile velocities. The objective of this thesis has been to develop the standard compatible channel estimation algorithms for the 3G mobile communication systems.

The time-varying characteristics of wireless communication channels along with some commonly used channel models have been investigated with an emphasis on a class of small-scale fading channels and Clarke's Rayleigh fading model. Some numerical results concerning the Rayleigh fading channel have also been obtained through the modelling and simulation of the channel for different mobile velocities.

The maximum likelihood estimator and its variations including pilot-assisted and decision-directed estimation algorithms have been analyzed and simulated. The Bhattacharyya bound of the BER performance for both downlink and uplink of WCDMA systems have been studied. It has been shown that under certain conditions, the downlink using the time-multiplexed pilot symbols and the uplink utilizing the code-multiplexed pilot symbols have equivalent BER performance.

Data-aided channel estimation methods have been classified into two categories ? pilot-assisted techniques and decision-directed ones. Pilot-assisted algorithms are reliable and accurate for slow-fading channels, but they cannot track well fast-fading channels. On the other hand, decision-directed estimation is suitable for fast fading environments, but it suffers from the decision error problem.

A two-stage channel estimation scheme for both the downlink and the uplink of WCDMA systems has been proposed based on the existing WMSA approach. The new technique has combined the pilot-assisted and decision-directed schemes and has been able to provide a superior estimation performance over the basic WMSA approach. A simulation study of the proposed estimation method has been undertaken, showing both the estimated channel characteristics and the BER performance of the WCDMA system for different mobile velocities and confirming the effectiveness of the proposed two-stage strategy.

An adaptive transversal filter in conjunction with the least mean square algorithm has been applied to WCDMA channel estimation. A theoretical analysis of the mean square error of the LMS algorithm has been carried out, revealing the superiority of a variable step-size update mechanism in convergence speed over the conventional fixed step-size scheme. An easy-to-implement yet efficient two-stage update scheme using different step-sizes has been proposed. It has been shown that a fast convergence speed can be achieved by using a large step-size at an early stage of the adaptive filtering, and in the mean time, the steady-state error can be reduced to a satisfactory degree by employing a

small step-size at a late stage of the update algorithm. The proposed method has been simulated and compared with the conventional constant step-size adaptive algorithm for WCDMA uplink channel estimation. Computer simulations have shown that the proposed method outperforms the conventional fixed step-size LMS adaptive algorithm.

6.2 Suggestions for Future Work

Adaptive channel estimation is a promising technique in wireless communications. The LMS adaptive algorithm with variable step-size has been studied in this thesis. Other adaptive filtering methods such as the normalized LMS, the recursive least square (RLS), the lattice structure and IIR adaptive filters will be investigated in the future with a focus on variable step-size schemes.

In this thesis, single-user WCDMA communication systems with three multipaths have been considered for computer simulations and performance study. However, there exist multiple users in practical WCDMA communication systems where one user would suffer more or less interference from another. In order to realize an optimal receiver, the interferences from other users should be taken into account. Therefore, the issue of channel estimation for multiuser WCDMA systems will be addressed in future study. An efficient approach is to combine the data-aided channel estimation techniques with multiuser detection. There might be different ways to pursue in this aspect. One way is to implement the channel estimation first and then formulate multiuser detection algorithms based on the estimated channel characteristics. Another combination scheme could be to

carry out interference cancellation as usually done in multiuser detection and then implement accurate channel estimation for Rake combining in the receiver. More investigations and experimentations will be needed to optimize the overall combination scheme.

Appendix A

WCDMA Downlink and Uplink Physical Channels

Table A.1 Downlink physical channels of WCDMA

Channel Type		Main function
Dedicated channel (DCH)	Dedicated control channel	Carry control information
	Dedicated data cannel	Carry data information
Common pilot channel (CPICH)	Primary CPICH	Reference for other downlink channels
	Secondary CPICH	Reference for the Secondary CCPCH and the downlink DPCH
Common control channel (CCPCH)	Primary CCPCH	Carry the BCH transport channel
	Secondary CCPCH	Carry the FACH and PCH
Synchronization channel (SCH)	Primary SCH	Synchronization
	Secondary SCH	Synchronization
Physical downlink shared channel (PDSCH)		Carry the downlink shared channel transport channel
Acquisition indicator channel (AICH)		Carry Acquisition indicators (AIs)
Access preamble acquisition indicator channel (AP-AICH)		Carry AP acquisition indicators (API) of CPCH.
Collision detection/channel assignment indicator channel (CD/CAICH)		Carry CD indicator
Paging indicator channel (PICH)		Carry the paging indicators (PI)
CPCH Status indicator channel (CSICH)		Carry CPCH status information

Table A.2 Uplink physical channels of WCDMA

Channel Type		Main function
Dedicated channel (DCH)	Dedicated control channel	Carry control information
	Dedicated data cannel	Carry data information
Common physical channel	Physical random access channel (PRACH)	Carry the RACH
	Physical common packet channel (PCPCH)	Carry the CPCH

Appendix B

Uplink DPDCH and DPCCH Fields

Table B.1 Uplink DPDCH fields

Slot Format #i	Channel Bit Rate (kbps)	Channel Symbol Rate (ksps)	SF	Bits/slot	N_{data}
0	15	15	256	10	10
1	30	30	128	20	20
2	60	60	64	40	40
3	120	120	32	80	80
4	240	240	16	160	160
5	480	480	8	320	320
6	960	960	4	640	640

Table B.2 Uplink DPCCH fields

Slot Format #i	Channel Bit Rate(kbps)	SF	Bits/slot	N_{pilot}	N_{TPC}	N_{TFCI}	N_{FBI}
0	15	256	10	6	2	2	0
0A	15	256	10	5	2	3	0
0B	15	256	10	4	2	4	0
1	15	256	10	8	2	0	0
2	15	256	10	5	2	2	1
2A	15	256	10	4	2	3	1
2B	15	256	10	3	2	4	1
3	15	256	10	7	2	0	1
4	15	256	10	6	2	0	2
5	15	256	10	5	1	2	2
5A	15	256	10	4	1	3	2
5B	15	256	10	3	1	4	2

Appendix C

Downlink DPCH Fields

Table C.1 Downlink DPDCH and DPCCH fields

Slot Format #i	Channel Bit Rate (kbps)	Channel Symbol Rate (ksps)	SF	Bits/slot	DPDCH Bits/slot		DPCCH Bits/slot		
					N_{data1}	N_{data2}	N_{TPC}	N_{TFCI}	N_{pilot}
0	15	7.5	512	10	0	4	2	0	4
0A	15	7.5	512	10	0	4	2	0	4
0B	30	15	256	20	0	8	4	0	8
1	15	7.5	512	10	0	2	2	2	4
1B	30	15	256	20	2	4	4	4	8
2	30	15	256	20	2	14	2	0	2
2A	30	15	256	20	4	14	2	0	2
2B	60	30	128	40	2	28	4	0	4
3	30	15	256	20	2	12	2	2	2
3A	30	15	256	20	4	10	2	4	2
3B	60	30	128	40	2	24	4	4	4
4	30	15	256	20	2	12	2	0	4
4A	30	15	256	20	2	12	2	0	4
4B	30	30	128	40	4	24	4	0	8
5	30	15	256	20	2	10	2	2	4
5A	30	15	256	20	2	8	2	4	4
5B	60	30	128	40	4	20	4	4	8
6	30	15	256	20	2	8	2	0	8
6A	30	15	256	20	2	8	2	0	8
6B	60	30	128	40	4	16	4	0	16
7	30	15	256	20	2	6	2	2	8
7A	30	15	256	20	2	4	2	4	8
7B	60	30	128	40	4	12	4	4	16
8	60	30	128	40	6	28	2	0	4
8A	60	30	128	40	6	28	2	0	4
8B	120	60	64	80	12	54	4	0	8

Table C.1 Continued

Slot Format #i	Channel Bit Rate (kbps)	Channel Symbol Rate (ksps)	SF	Bits/slot	DPDCH Bits/slot		DPCCH Bits/slot		
					N_{data1}	N_{data2}	N_{TPC}	N_{TFCI}	N_{pilot}
9	60	30	128	40	6	26	2	2	4
9A	60	30	128	40	6	24	2	4	4
9B	120	60	64	80	12	52	4	4	8
10	60	30	128	40	6	24	2	0	8
10A	60	30	128	40	6	24	2	0	8
10B	120	60	64	80	12	48	4	0	16
11	60	30	128	40	6	22	2	2	8
11A	60	30	128	40	6	20	2	4	8
11B	120	60	64	80	12	44	4	4	16
12	120	60	64	80	12	48	4	8	8
12A	120	60	64	80	12	40	4	16	8
12B	240	120	32	160	24	96	8	16	16
13	240	120	32	160	28	112	4	8	8
13A	240	120	32	160	28	104	4	16	8
13B	480	240	16	320	56	224	8	16	16
14	480	240	16	320	56	232	8	8	16
14A	480	240	16	320	56	224	8	16	16
14B	960	480	8	640	112	464	16	16	32
15	960	480	8	640	488	488	8	8	16
15A	960	480	8	640	480	480	8	16	16
15B	1920	960	4	1280	976	976	16	16	32
16	1920	960	4	1280	1000	1000	8	8	16
16A	1920	960	4	1280	992	992	8	16	16

References

[1] Rapport T. S., *Wireless Communications*, Prentice Hall, Upper Saddle River, New Jersey, 2002.

[2] Van Rees J., "Measurements of the wideband radio channel characteristics for rural, residential and suburban areas", *IEEE Transactions on Vehicular Technology*, Vol. VT-36, No.2, pp. 1-6, Feb. 1987.

[3] Seidel S. Y., Jain. S., Lord M. and Singh R., "Path loss, scattering and multipath delay statistics in four European cities for digital cellular and micro cellular radio telephone", *IEEE Transactions on Vehicular Technology*, Vol. 40, No.4, pp. 721-730, Nov. 1991.

[4] Price R. and Green P.E., "A communication technique for multipath channel", *Proceedings of the IRE*, Vol.46, pp. 555-570, Mar. 1958.

[5] John G. Proakis, *Digital Communications,* McGraw-Hill, U.S.A, 1998.

[6] Jakes W., *Microwave Mobile Communications,* John Wiley & Sons, 1974.

[7] Harri Holma and Antti Toskala, *WCDMA for UMTS: Radio Access for Third Generation Mobile Communications,* John Wiley & Sons, 2000.

[8] Bernard Sklar, *Digital Communications: Fundamentals and Applications,* Prentice Hall, Upper Saddle River, New Jersey, 2001.

[9] Smith J. I., "A computer generated multipath fading simulation for mobile radio", *IEEE Transaction on Vehicular Technology*, Vol. VT-24, No. 3, pp. 39-40, Aug.

1975.

[10] A. V. Oppenheim and R. W. Schafer, *Discrete-time Signal Processing,* Prentice Hall, New Jersey, 1998.

[11] ETSI TS 125 211 V3.2.0 (2000-03): Universal Mobile Telecommunications System (UMTS); Physical channels and mapping of transport channels onto physical channels (FDA) (3G TS 25.211 version 3.2.0 Release 1999).

[12] Heinrich Meyr, Marc Moeneclaey and Stefan A. Fechtel, *Digital Communication Receivers: Synchronization, Channel Estimation, and Signal Processing,* John Wiley & Sons, U.S.A., 1998.

[13] F. Ling, "Optimal reception, performance bound, and cutoff rate analysis of reference-assisted coherent CDMA communications with applications", *IEEE Transactions on Communications*, Vol. 47, No. 10, pp. 1583-1592, Oct. 1999.

[14] Jyh-Hau. C. and Yumin Lee, "Joint synchronization, channel length estimation, and channel estimation for the maximum likelihood sequence estimator for high speed wireless communications", *IEEE Proceedings*, Vol.3, pp.1535-1539, Sept. 2002.

[15] F. Ling, "Coherent detection with reference-symbol based channel estimation for direct sequence CDMA uplink communications", *The 43rd 1993 IEEE Vehicular Technology Conference*, pp. 400-403, May 1993.

[16] F. Ling, "Pilot assisted coherent DS-CDMA reverse link communications with optimal robust channel estimation", *IEEE International Conference on Acoustics, Speech, and Signal Processing*, Vol.1, pp.263 - 266 Apr. 1997.

[17] A. Papoulis, *Probability, Random Variables and Stochastic processes,* New York: McGraw-Hill, 1984.

[18] Simon Haykin, *Adaptive Filter Theory,* Prentice Hall, Upper saddle River, New Jersey, 2002.

[19] Andrew J. Viterbi, *CDMA Principles of Spread Spectrum Communication,* Addison Wsley, 1995.

[20] M. K. et al., *Spread Spectrum Communications Handbook,* McGraw-Hill, New York, 1994.

[21] D. Divasalar and M. K. Simon, "The design of trellis coded MPSK for fading channels: performance criteria", *IEEE Transactions on Communications*, Vol. 36, No.9, pp. 1004-1012, Sept.1988.

[22] Gordon J. R. Povey and Peter M. Grant, "A decision-directed spread-spectrum Rake receiver for fast fading mobile channels", *IEEE Transactions on Vehicular Technology,* Vol. 45. No. 3, pp.491-502, Aug. 1996.

[23] Petri K. and Ville H., "Adaptive filtering for fading channel estimation in WCDMA downlink", *The 11th IEEE International Symposium on Indoor and Mobile Radio Communications*, Vol.1, pp.549-553, Sept. 2000.

[24] Ji-Woong Choi and Yong-Hwan Lee, "An adaptive channel estimator in pilot channel based DS-CDMA system", *The 55th IEEE Vehicular Technology Conference*, Vol.3, pp.1429-1433, May 2002.

[25] Ji-Woong Choi and Yong-Hwan Lee, "Adaptive channel estimation in DS-CDMA

downlink systems", *The 13th IEEE International Symposium on Indoor and Mobile Radio Communications*, Vol.3, pp.1432-1436, Sept. 2002.

[26] Lars Lindbom, Mikael Sternad and Anders Ahlen, "Tracking of time-varying mobile radio channels—part I: the Wiener LMS algorithm", *IEEE Transactions on Communications,* Vol. 49, No. 12, pp.2207-2217, Dec., 2001.

[27] Mikael Sternad, Lars Lindbom, and Anders Ahlen, "Wiener design of adaptation algorithms with time-invariant gains", *IEEE Transactions on Signal Processing,* Vol. 50, No. 8, pp.1895-1907, Aug. 2002.

[28] A. Mammela, and V. P. Kaasila, "Prediction, smoothing and interpolation in adaptive diversity reception", *IEEE International Symposium on Spread Spectrum Techniques & Applications*, Vol.2, pp.475-478, Jul. 1994.

[29] V. P. Kaasila and A. Mammela, "Bit-error probability for an adaptive diversity receiver in a Rayleigh-fading channel", *IEEE Transactions on Communications,* Vol. 46, No. 9, pp. 1106-1108, Sept.1998.

[30] P. Y. Kam, "Optimal detection of digital data over the nonselective Rayleigh fading channel with diversity reception", *IEEE Transaction on Communications*, Vol.39, No.2, pp. 214-219, Feb.1991.

[31] L. B. Milstein, "Interference rejection techniques in spread spectrum communications", *IEEE Proceedings,* Vol.76, pp.657-671, Jun. 1988.

[32] K. Wesolowski, C. M. Zhao and W. Rupprecht, "Adaptive LMS transversal filters with controlled length", *IEE Proceedings on Radar and Signal Processing*, Vol.139,

pp.233-238, Jun. 1992.

[33] Paulo S. R. Diniz, *Adaptive Filtering: Algorithms and Practical Implementation,* Kluwer Academic Publisher Group, 2002.

[34] Lars L., Jonas R., Anders A. and Mikael S., "Automatic tuning of the step size in WLMS algorithm: applications to EDGE", *The 56th IEEE Vehicular Technology Conference*, Vol.4, pp.2229-2233, Sept. 2002.

[35] 3GTS 25.101 V3.3.1 (2000-06): 3rd Gerneration Partnership Project; Technical Specification Group Radio Access Networks; UE Radio transmission and Reception (FDA) (Release 1999).

[36] Irvine Garrick T. and McLaine Peter J., "Symbol-aided plus decision-directed reception for PSK/TCM modulation on shadowed mobile satellite fading channels", *IEEE Journal on Selected Areas in Communications,* Vol. 10, No. 8, pp. 1289-1299, Oct. 1992.

[37] Anna Zhuang and Markku R., "Combined pilot aided and decision directed channel estimation for the Rake receiver", *The 52nd IEEE Vehicular Technology Conference*, Vol. 2, pp.710-713, Sept. 2000.

[38] H. Andoh, M. Sawahashi and Adachi F., "Channel estimation filter using time-multiplexed pilot channel for coherent Rake combing in DS-CDMA mobile radio", *IEICE Transactions on communications,* Vol. E81-B, No. 7, pp.1517-1525, Jul. 1998.

[39] Adachi F., M. Sawahashi and H. Suda, "Wideband DS-CDMA for next-generation

mobile communication systems", *IEEE Communications Magazine*, Vol.36, No.9, pp. 56-69, Sept. 1998.

[40] M. L. Mother and J. H. Lodge, "TCMP-a modulation and coding strategy for Rician fading channel", *IEEE Journal on Selected Areas in Communications*, Vol.7, No.9, pp. 1347-1355, Dec. 1989.

[41] J. K. cavers, "An analysis of pilot symbol assisted modulation for Rayleigh fading channels", *IEEE Transactions on Vehicular Technique*, Vol.40, No.4, pp.689-693, Nov. 1993.

[42] Y. Honda and K. Jamal, "Channel estimation based on time-multiplexed pilot symbols", *IEICE Technical Report*, RCS96-70, Aug. 1996.

[43] G. B. Giannkis, Y. Hua, P. Stoica and L. Tong, *Signal Processing Advances in Wireless and Mobile Communications,* Prentice Hall, Upper Saddle River, New Jersey, 2001.

[44] P. M. Crespo and J. Jimenez, "Computer simulation of radio channels using a harmonic decomposition technique", *IEEE Transactions on Vehicular Technology* , Vol. 44, No. 3, pp. 411-419, Aug. 1995.

[45] E. De Carvalho and D. T. M. Slock, "Cramer-Rao bounds for semi-blind and training sequence based channel estimation", The 1st IEEE Signal Processing Workshop on Signal Processing Advances in Wireless Communications, pp.129-132, April 1997.

[46] H. Andoh, M. Sawahashi and Adachi F., "Performance comparison between

time-multiplexed pilot channel and parallel channel for coherent Rake combining in DS-CDMA mobile radio", *IEICE Transactions on Communications,* Vol. E81-B, No. 7, pp.1417-1425, Jul. 1998.

[47] Lee, W. C. Y., "Elements of cellular mobile radio systems", *IEEE Transactions on Vehicular Technology,* Vol.V-35, No.5, pp. 48-56, May 1986.

[48] YanZhang, *Carrier Phase and Frequency Estimation for Burst-Mode Communications,* A Master Thesis of Concordia University, 2001.

[49] M. Benthin and K, Kammeyer, "Influence of channel estimation on the performance of a coherent DS-CDMA system," *IEEE Transactions on Vehicular Technology,* Vol.46, No.2, pp. 262-267, May 1997.

[50] K. Pahlavan and J.W. Matthews, "Performance of adaptive matched filter receivers over fading multipath channels," *IEEE Transactions on Communications,* Vol.38, No.12, pp. 2106-52113, December 1990.

[51] Xi-Bin Han and Wei-Ping Zhu, "Variable step-size adaptive channel estimation for WCDMA receiver," *International Symposium on Intelligent Multimedia, Video and Speech Processing*, Hong Kong, China, October 2004.

[52] Xi-Bin Han and Wei-Ping Zhu, "Wide-band CDMA channel estimation: a data-aided multi-slot averaging method," *IEEE Mid-West Circuits and Systems Symposium*, Hiroshima, Japan, July 2004.